The Andrzej Soltan Institute for Nuclear Studies

Setup and Optimisation of the Muon Trigger System for the ZEUS Backing Calorimeter

Paweł Pluciński

Thesis submitted in partial fulfilment of the
requirements for the Ph.D. degree in Physics.
Prepared under supervision of
prof. dr hab. Aleksander Filip Żarnecki

Warszawa 2007

"Nothing travels faster than the speed of light with possible exception of bad news, which obeys its own special laws".

Douglas Adams

Abstract

The ZEUS experiment is one of the two experiments at the HERA collider operating at DESY, Hamburg. HERA collides electrons or positrons with protons at the center of mass energy of up to 318 GeV. The main aim of the experiment is to study the structure of proton in the process of Deep Inelastic Scattering (DIS), but a variety of other phenomena can also be studied, including searches for "new physics" beyond the Standard Model. One of the biggest components of the ZEUS detector is the so called Backing Calorimeter (BAC) which was designed, built and operated for 15 years by a group of Polish physicists and engineers.

One of the most important results from HERA 1994-2000 running was the excess of events with jet and high-p_T isolated leptons reported by H1, but not confirmed by ZEUS. Therefore, an important goal of the ZEUS detector upgrade in 2000-2002 was to increase the efficiency of muon identification on the trigger level. This was obtained by implementing the muon trigger in the Backing Calorimeter.

The thesis summarize the work which was done in years 2000 to 2006. Subsequent phases of the BAC muon trigger setup, startup and optimization are described. Dedicated diagnostics system has been developed to monitor performance of the trigger system on all hardware and software levels. Detailed information about the status of system components can be used to select optimum configuration parameters. Information stored in the database is also used to reproduce performance of the BAC muon trigger in the ZEUS Monte Carlo.

Analysis based on the ZEUS data collected in 2005 shows that, in the regions where there were no major hardware problems, BAC trigger selection efficiency for high momentum muons is about 70 to 80%. Results are well reproduced by Monte Carlo confirming that performance of the BAC muon trigger is well understood. By including BAC muon trigger in the ZEUS trigger system efficiency for high-mass di-muon event selection was increased by about 20%.

Contents

Chapter 1

Introduction

The trigger systems plays a crucial role in High Energy Physics (HEP) experiments. One of the main goals of current and future HEP experiments is to search for rare phenomena within and beyond the Standard Model (SM). With increasing energies of colliding beams, cross sections for particle interactions decrease and we have to collide beams with higher and higher intensities. As a result, the background levels increase. The main aim of the trigger systems is to recognize events which should be collected and to reject background events which are not produced by beam-beam collisions (beam gas, cosmic rays, etc). In addition, there is a huge part of events which are produced by beam collisions but are not interesting from physics analysis point of view. In order to not overload the readout system of the experiment and due to limited capacity of the data storage system, the trigger system is intended to reject such events as well. Similar to others collider experiments, the trigger of the ZEUS experiment was designed as a multi-level system, consisting of three levels with increasing selectivity.

The "Hadron Electron Ring Accelerator" (HERA) was built at DESY, Hamburg mainly to study the structure of the proton in the new kinematic domain, not accessible in the fixed target experiments. It collided electrons or positrons with protons at the center of mass energy of up to 318 GeV. The machine also enabled us to study a variety of different phenomena from elastic and diffractive processes to searches for "new physics" beyond the Standard Model. The ZEUS experiment is one of the two $e^{\pm}p$ experiments at HERA. One of its biggest components is the so called Backing Calorimeter (BAC) which was designed and built by a group of Polish physicists and engineers.

In the years 2000-2002 a major of upgrade of the machine and of the ZEUS detector took place. One of the important goals of the detector upgrade was to increase the efficiency of muon identification on the trigger level. This was obtained by implementing the muon trigger in the Backing Calorimeter

position readout.

This thesis present the design and implementation of the Backing Calorimeter muon trigger, and describe its setup, optimization and performance. After the brief description of the HERA collider and ZEUS experiment in chapters 2 and 3, trigger system and ZEUS data acquisition chain are presented in chapter 4. The mechanical design and the readout structure of the ZEUS Backing Calorimeter is described in chapter 5. The design of the BAC muon trigger is also presented in details. In order to startup the trigger, and also to achieve optimum performance of the trigger system, dedicated diagnostic system and optimization procedure has been developed. The idea, implementation, results of various electronics test as well as the description of the optimization procedure can be found in chapter 6. In order to verify the quality of the trigger data, trigger efficiency studies were performed. Methods used for performance studies and obtained results are described in chapter 7. Most of results presented in chapters 6 and 7 were obtained by the author of this thesis. Final conclusions are given in chapter 8.

Chapter 2

The Electron-Proton Collider HERA

2.1 Overview of the machine

The HERA (Hadron Electron Ring Anlage) accelerator was built in the Deutches Elektronen-SYnchrotron laboratory (DESY,Hamburg) as the first electron (and positron) - proton ($e^{\pm}p$) collider in the world [1]. HERA opened possibilities to study the structure of the proton,in the new kinematic range and allowed us to test the Standard Model of the Particle Physics and to search phenomena beyond that model in a unique environment.

The construction of HERA started in 1985 and took 6 years. The first ($e^{\pm}p$) collision were observed in 1991 but the first data for physics analysis were taken in 1992. The collider consists of two rings of 6.5 km circumference located 10 to 25 m under earth surface in Hamburger Volkspark (see Figure 2.1). The first ring is used to accumulate and accelerate protons, while the second one is used for electrons or positrons. The proton ring has been equipped with superconducting dipole magnets operating at a temperature of 4.2 K producing a magnetic field of 4.7 Tesla. The magnets of the electron ring are normal conducting, operating at room temperature, as the required magnetic field is only about 0.15 Tesla.

Schematic view of the HERA accelerator complex is presented in Figure 2.2 Protons are pre-accelerated to an energy of 50 MeV in proton-LINAC and then accelerated in DESY3 to an energy of 7.5 GeV. From DESY3 protons are injected to PETRA and then at energy of 37 GeV to HERA proton ring. Electrons are pre-accelerated in linear accelerators LINAC1 and DESY2 to an energy of 220 MeV and 7.5 GeV. Before injection into HERA electrons and positrons are accelerated in PETRA to an energy of 14 GeV.

Figure 2.1: HERA (Hadron Electron Ring Anlage)

The HERA collider was designed to accelerate protons to an energy of 820 GeV and electrons or positrons to 30 GeV. Due to beam intensity limitations electron beam energy was limited to 27.6 GeV. However, starting from year 1998 the proton beam energy was increased to 920 GeV, so the designed center of mass energy was obtained.

The beams circulating in opposite directions collide in two interaction regions where experimental halls were built. The ZEUS [2] detector is situated in the South Hall and the H1 [3] in the North Hall. In addition to the H1 and ZEUS experiments designed to study $(e^{\pm}p)$ collisions, two additional experiments HERMES [4] and HERA-B [5], located in the East and West halls, respectively, were designed as the fixed-target experiments. The main aim was to investigate the spin structure of the nucleon (HERMES) and to study the CP-violation in $B^0 B^0$ system (HERA-B).

The data collected until 2000 resulted in a tremendous improvement in the knowledge of the proton structure functions. However, HERA physics turned out to be more rich and fruitful than expected. Data analysis resulted in tens of publications covering large variety of subjects, ranging from quasi-elastic vector meson production to multi-jet cross section measurements and limits on the quark radius. In addition some interesting events were observed, in particular excess of high-Q^2 events or the excess of events with jet and high-p_T isolated leptons [6]. These events were considered as possible signature of "new physics" beyond the Standard Model like the sub-structure of quarks or violation of the lepton number conservation.
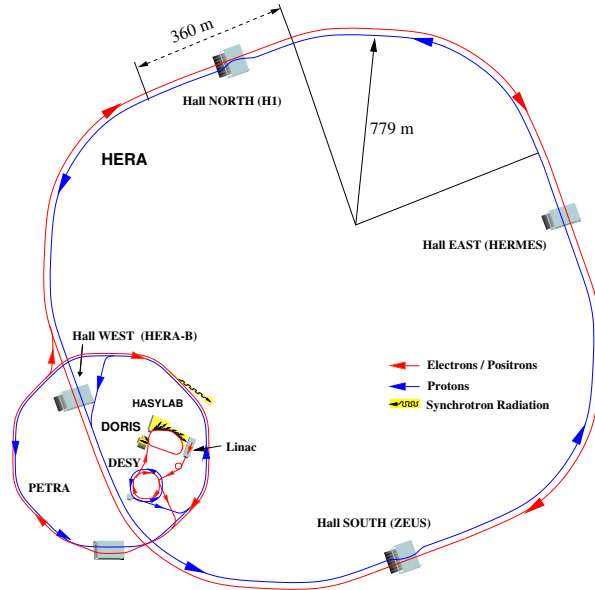
Figure 2.2: The Hera (Hadron Electron Ring Anlage)

In order to confirm or reject these hypothesis higher statistic needed. Therefore, in period from 2000-2002 upgrade of HERA collider took place giving an opportunity to increase the luminosity of colliding beams. The aim of the upgrade was to deliver about 1 fb^{-1} per experiment until 2005. Unfortunately the startup of the machine after upgrade was very slow (see Figure 2.3) and eventually both experiments collected only about 0.5 fb^{-1}.

2.2 Electron-Proton Physics at HERA

Deep Inelastic Scattering

The HERA accelerator as the first electron (or positron) - proton collider in the world was dedicated to study of the structure of the proton in the processes of Deep Inelastic Scattering (DIS). Electron-proton scattering is considered as a DIS process when there is a large four-momentum transfer between scattering particles and hadronic final state with large invariant mass (much larger than the proton mass) is produced. DIS processes can be divided into two categories: Neutral Current (NC) process with Z^o or γ exchange and Charged Current (CC) process with W^+ or W^- exchange. In the Quark-Parton Model (QPM) they are described as electron scattering off one of the quarks or antiquarks in the proton (see Figure 2.4).

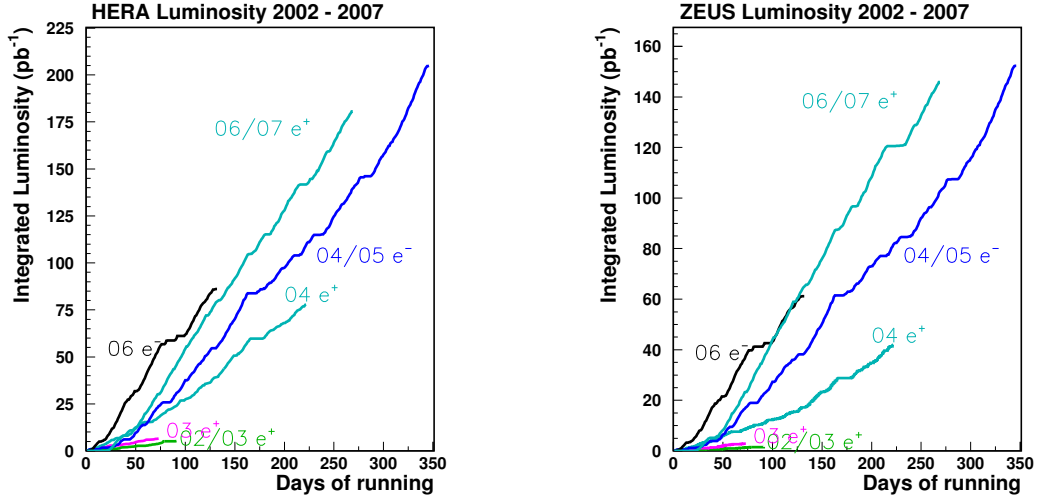In the kinematic description of the DIS events following four-momenta

Figure 2.3: Integrated luminosity delivered by HERA in period from 2002 till 2007 (left plot) and the one taken with ZEUS detector (right plot)

are considered:

- k - the four-momenta of incoming electron

- $k^{'}$ - the four momenta of scattered lepton (electron or neutrino)

- P - the four-momenta of incoming proton

- q - the four-momentum transfer between lepton and proton

Using these four-momenta following Lorenz-invariant variables are introduced to describe DIS events:

- the value of the four-momentum transfer squared

$$Q^2 \;\; = \;\; -q^2 = -(k - k^{'})^2$$

- Bjorken scaling variable x

$$x \;\; = \;\; \frac{-q^2}{2q \cdot P}$$

In the parton model x is interpreted as a fraction of proton momentum carried by a struck parton, in the infinite proton momentum reference frame, when the proton mass can be neglected.
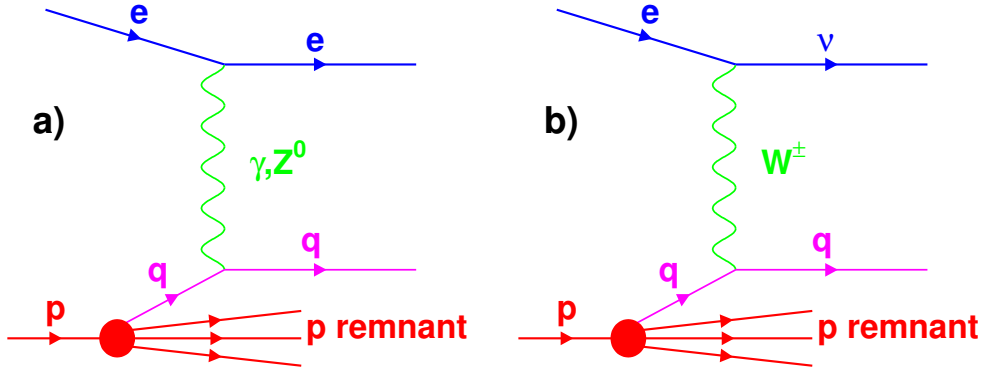
Figure 2.4: Leading order Feynman graphs for deep inelastic ep scattering: (a) for NC and (b) for CC reactions. Note that scattering on antiquarks is also possible.

- Bjorken variable y

$$y = \frac{q \cdot P}{k \cdot P}$$

  In the proton rest frame y corresponds to the fraction of initial electron energy transfered to the proton.

The above variables are not independent and can be related by the following equation:

$$Q^2 = x \cdot y \cdot s$$

where s is the ep center of mass energy defined as:

$$s = \sqrt{k + P}$$

The cross section for NC DIS can be written in terms of the so called structure functions of the proton F_2, F_3 and F_L, and the variables x,y and Q^2:

$$\frac{d^2\sigma_{NC}^{e^\pm p}}{dxdQ^2} = \frac{2\pi\alpha^2}{xQ^4}\left[Y_+ F_2^{\gamma Z}(x,Q^2) \mp Y_- x F_3^{\gamma Z}(x,Q^2) - y^2 F_L^{\gamma Z}(x,Q^2)\right],$$

where α denotes the electromagnetic coupling constant and $Y_\pm = 1\pm(1-y)^2$. The NC structure functions are the same for the e^-p and e^+p scattering. The difference in the scattering cross section resulting from Z^0 exchange is taken

into account in the xF_3 contribution, which changes sign with charge of the scattered lepton. F_L is called a longitudinal structure function. At low Q^2, $Q^2 \ll M_Z^2$, only photon exchange is relevant and dominant contribution to the NC ep DIS is described by the structure function F_2. In the QPM it is related to the quark and antiquark distributions in the proton:

$$F_2^\gamma(x, Q^2) = \sum_q x e_q^2 [q(x, Q^2) + \bar{q}(x, Q^2)],$$

where $q(x, Q^2)$ and $\bar{q}(x, Q^2)$ are the quark and antiquark momentum distribution functions in the proton.

Measurements of the NC and CC DIS cross sections analyzed within the perturbative QCD framework allow us to determine the quark and gluon momentum distributions in the proton. Before HERA, structure functions were measured by fixed target experiments only for Q^2 values up to about 100 GeV^2. At HERA measurement of the proton structure functions up to $Q^2 \sim 10^5$ GeV^2 is possible.

Lepton Pair Production

To optimize BAC muon trigger setup and study its performance the di-muon sample of events was used. These events are produced in two main channels: production and decay of J/Ψ mesons and the so called Bethe-Heitler process. Most of J/Ψ mesons are produced in the quasi-elastic process, when a photon emitted from electron fluctuates into the vector meson state and the proton remains intact. In the perturbative QCD this process is described by exchange of a gluon pair (see Figure 2.5). Production of J/Ψ mesons can be studied in the DIS region, but the cross section is highest in the region of very low Q^2, when the scattered photon is almost real (so called photoproduction). Muon pairs from J/Ψ decays are characterized by a narrow peak in the invariant mass distribution, corresponding to the meson mass of 3.1 GeV.

In addition to the "resonant" contribution coming from J/Ψ decays, muon pairs with arbitrary (even very large) invariant masses can be produced in the so called Bethe-Heitler process. Photon emitted from incoming electron interacts with another photon emitted by the proton and a lepton-antilepton pair with back-to-back topology is produced (see Figure 2.6). Also in this case, photon remains intact for most events.
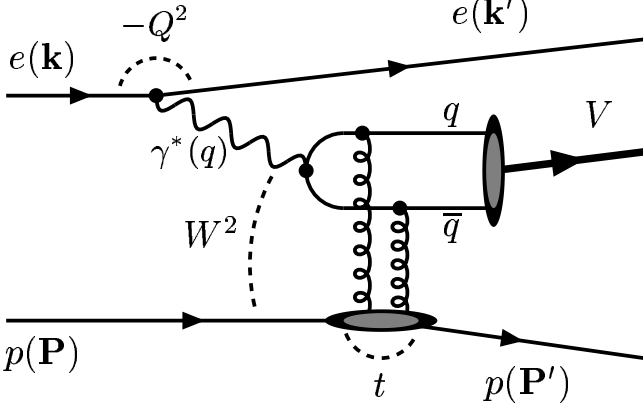
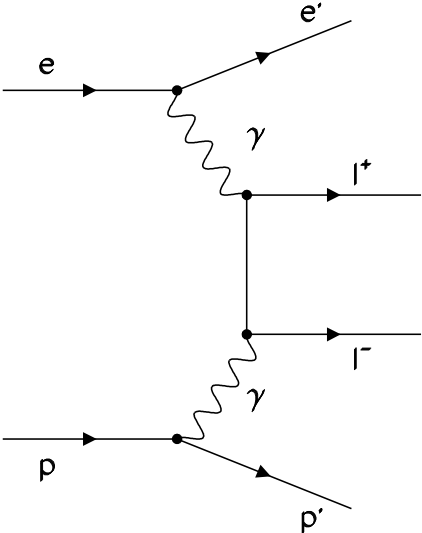Figure 2.5: Leading order Feynman diagram for vector meson (V) production in *ep* scattering at HERA.

Figure 2.6: Leading order Feynman diagram for lepton pair production in Bethe-Heitler process at HERA.

Chapter 3

ZEUS Experiment

The ZEUS experiment [2] is composed of several specialized subcomponents surrounding the nominal interaction point (IP). Contrary to other collider experiments at LEP, Tevatron or LHC the ep center of the mass frame is moving w.r.t the laboratory frame with large Lorentz boost ($\gamma \sim 3$) in the proton beam direction. For that reason ZEUS detector is asymmetric, more detectors element and absorbers are located in the forward direction than in the rear one. In this chapter, main components of the ZEUS detector are briefly described. The schematic view of the detector, with indicated location of detector components is presented in Figure 3.1.

In 2000-2002 upgrade of ZEUS experiment took place. The main goal of the detector modernization was to exploit the new capabilities given by the increased luminosity of HERA collider. Close to the interaction point, the new Silicon Microvertex Detector (MVD) was installed. The MVD detector allows to measure with high accuracy the position of the primary and secondary verticles. Precise vertexing is of special importance for studies of heavy quark production at HERA. ZEUS detector had not been equipped with the vertex detector since 1997 when the first vertex detector was switched off due to significant efficiency losses.

In order to improve reconstruction of charged particles produced in the foward direction a new Straw Tube Tracker (STT) was also installed. Moreover, many existing detector components were modified or equipped with the new readout electronics and trigger system to allow for higher data taking efficiency. The main aim of the Backing Calorimeter upgrade was to increase the efficiency of muon finding in the ZEUS experiment. For that purpose muon trigger system was installed.

For the description of the ZEUS detector and data analysis a right-handed coordinate system is used with Z axis pointing into the proton beam direction (referred to as "forward") and the X axis horizontal, pointing towards
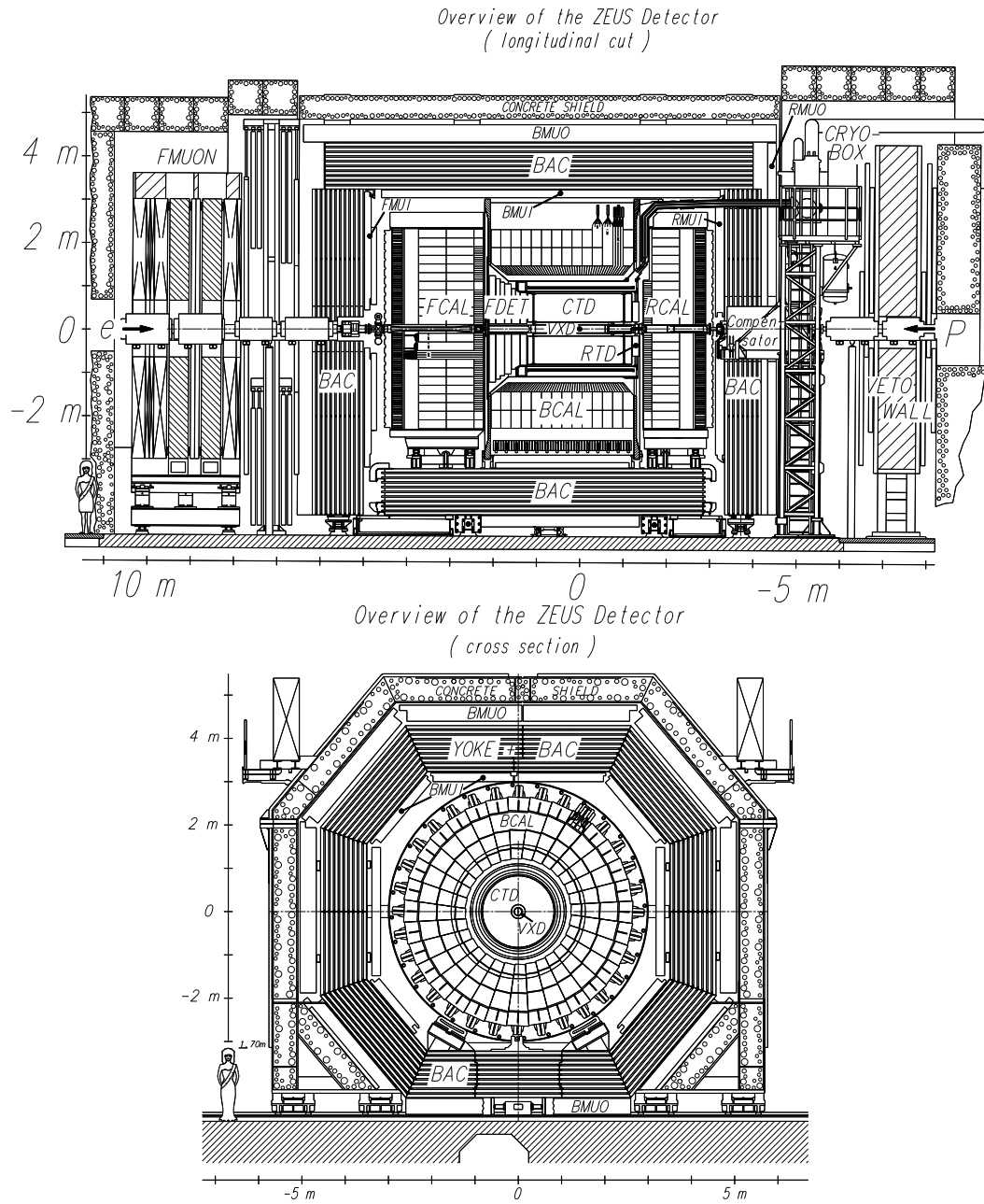
Figure 3.1: Cross section of the ZEUS detector along the beam axis (upper plot) and perpendicular to the beam (lower plot)
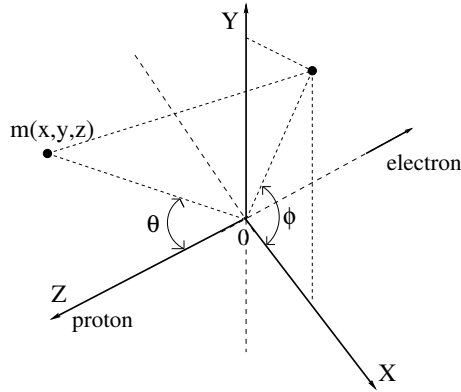
Figure 3.2: The coordinate system of the ZEUS detector is a right-handed system with the Z axis pointing into the proton beam direction, while the X axis into the centre of HERA.

the centre of HERA (see Figure 3.2). The electron beam direction is referred to as "rear".

3.1 Silicon Microvertex Detector

For the precise reconstruction of observed ep collisions accurate determination of the actual interaction point position is very important. As in most collider experiments, dedicated device was designed for this purpose. The first version of the ZEUS Vertex Detector (VXD) was installed in 1991. Due to hardware problems caused by synchrotron radiation the VXD detector was switched off and finally removed.

In order to keep the possibility of the vertex position measurement with high accuracy new Silicon Microvertex Detector [7] has been installed in 2000/01 shutdown. The detector consists of a 65 cm long "Barrel" part with 3 layers of Si sensors parallel to the beam. Each of these layers is composed of several carbonfibre supports and 5 Si modules called "Ladders". In the forward region there are 4 layers of Si detectors, perpendicular to the beam. Each layer consists of 14 modules mounted on a carbonfibre support, called a "wheel". The Silicon Microvertex allows to measure the position of the primary vertex with an accuracy of 10 μm. Moreover, secondary vertices, resulting eg. from heavy quark decays, can be reconstructed with high efficiency and similar precision.

3.2   Central Tracking Detector

The Central Tracking Detector (CTD) [8] allows to reconstruct tracks and determine momentum of charged particles produced in an ep collision, and offers the possibility to determine the vertex position as well. The CTD consists of cylindrical drift chambers filled with a mixture of Ar, CO_2, and ethane. The detector covers the polar angle θ region from $15°$ to $164°$ and full range of azimuthal angle ϕ. An inner radius of the detector is 18.2 cm and an outer radius is 79.4 cm. The Central Tracking Detector is placed in a magnetic field of 1.4T created by superconducting solenoid. From geometrical point of view the CTD is divided into 8 so called "octans", each extending over 45 degrees in azimuthal angle, and 9 cylindrical layers of drift cells, so called "superlayers". The single octans consist of 72 drift cells, each equipped with 8 sense wires. The position resolution in $r - \phi$ is 230 μm, and the resolution of the transverse momentum , assuming that charged particles cross all layers is:

$$\frac{\sigma(p_t)}{p_t} = \ 0.0058 \ \cdot \ p_t(\text{GeV}) \ \oplus \ 0.0065 \ \oplus \ \frac{0.0014}{p_t}, \qquad (3.1)$$

where the first term is due to the resolution in the hit position determination, the second term to smearing from multiple scattering within the CTD and the last term to multiple scattering before the CTD. With CTD measurements only the position of interaction point in X and Y can be obtain with resolution of 0.1 cm, and in Z with a resolution of 0.4 cm.

3.3   Forward and Rear Tracking Detectors

The role of the Forward Tracking Detector (FTD) and of the Rear Tracking Detector (RTD) is to measure tracks of charged particles in the polar angle region not covered by Central Tracking Detector. These detector are also used to improve track reconstruction in the overlap regions, where tracks do not cross all CTD superlayers.

In order to measure tracks and reconstruct momentum of charged particles in polar angle region from $7.5°$ to $28°$ the Forward Tracking Detector was installed. The detector consists of three sets of wire drift chambers placed next to the forward CTD endcap plane. Each set consists of three drift chambers with different wire orientation. The RTD consists of one wire chamber, placed behind the CTD and allows us to measure tracks in the polar angle region from $159°$ to $170°$. Together with CTD, Forward and Rear Tracking detectors cover the polar angle region from $7.5°$ to $170°$ and full azimuthal angle.

3.4 Uranium Calorimeter

From the point of view of its mechanical structure the ZEUS central calorime-
ter (CAL) [9] can be divided into three parts: Forward (FCAL) Barrel
(BCAL) and Rear (RCAL) calorimeters. Together they cover polar angle
range from 2.8 to 176° and full range in azimuthal angle, see Figure 3.3.

The CAL design was based on scintillator plates as an active medium
and uranium absorber. The uranium has one major advantage over other
passive materials: nuclear processes contributing in the development of the
hadronic cascade result in a large neutron yield. These neutrons can give
significant contribution to the observed light yield by elastic scattering on
protons in organic scintillator. By proper choice of uranium and scintillator
plate thicknesses the response of uranium-scintillator calorimeter to elec-
trons and hadrons with the same energy can be made the same. This is the
so called calorimeter compensation phenomena. Thanks to compensation,
hadronic energy resolution can be significantly improved, as fluctuations of
the electromagnetic component in the cascade do not influence the response.
Under test beam conditions the Uranium Calorimeter was shown to measure
the energy of single particles with resolution of $35\%/\sqrt{E}$ [GeV] for hadrons
and $18\%/\sqrt{E}$ [GeV] for electrons and photons.

The three calorimeter parts, FCAL, BCAL and RCAL, are subdivided
into modules. The modules are transversally separated into towers and the
towers are in turn longitudinally divided into electromagnetic (EMC) and
hadronic sections (HAC). The EMC and the HAC sections are further seg-
mented into cells. Each EMC section is segmented transversally into four (in
FCAL and BCAL) or two cells (in RCAL) for better electron identification
and position measurement. The HAC towers in the FCAL and the BCAL
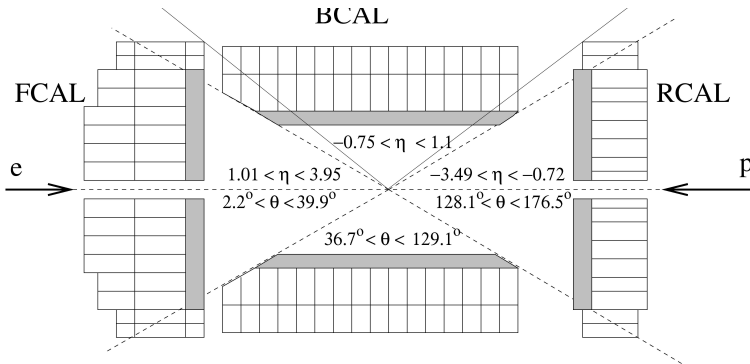are longitudinally subdivided into two hadronic cells (HAC1, HAC2).

Figure 3.3: Layout of the ZEUS Uranium Calorimeter.

3.5   Forward Muon Detector

The Forward Muon detector (FMUON) allows to determine momenta and production angle for muons emitted at small angles w.r.t the proton beam direction. The FMUON consists of 5 layers of streamer tubes, 4 planes of drift chambers and time of flight counter. The setup includes also two magnetized iron toroids required for momentum determination. The identification of the muon produced at IP requires matching of the signal detected in the chambers that are located inside the iron yoke with the track segment reconstructed in the chambers outside the yoke.

3.6   Barrel and Rear Muon Detectors

Barrel and Rear Muon chambers (BRMUON) [10] can be used to identify muons as well. Both detectors consist of two layers of streamer tubes, located inside and outside of the iron yoke. In addition to the return field of the central ZEUS solenoid, dedicated magnets are used to produce toroid magnetic field in the iron yoke. This field allows for the muon momenta measurement. For reconstruction of the muon momenta, track segments in both inner and outer chamber layers have to be reconstructed. For muon identification only, events with one track segment (in inner or outer layer) can also be used, although with smaller purity.

3.7   Backing Calorimeter

The Backing Calorimeter (BAC) was designed to improve energy measurement for hadronic showers that are not fully absorbed in high-precison central uranium calorimeter [11] and to identify muons. The BAC consists of iron plates of the detector yoke interleaved with aluminum proportional chambers. With this design, the energy of hadronic showers can be measured with resolution of the order of $100\%/\sqrt{E}$, as obtained under test-beam conditions for stand-alone BAC prototype.

The data collected until 2000 showed rather small statistics of hadronic cascades measured in the Backing Calorimeter, mainly due to the fact that the luminosity of colliding beams was not as high as expected. Moreover, the method used by the ZEUS Collaboration to reconstruct kinematic variables for NC DIS events (so called Double Angle method) does not require hadronic final state energy measurement. Thus, the main role of the Backing Calorimeter was to identify muons.

In the years 2000-2002 a major of upgrade of the HERA machine and of the ZEUS detector took place. One of the important goals of the detector upgrade was to increase the efficiency of muon identification on the trigger level. This was obtained by implementing the muon trigger in the Backing Calorimeter digital readout [12, 13]. More details about BAC design and muon trigger implementation will be given in chapter 5.

Chapter 4

Trigger and Data Acquisition

The distance between two subsequent bunches in electron and proton beams correspond to the time interval between two collisions of 96 ns. The resulting collision rate is about 10 MHz. All components of the ZEUS experiment read out signal from the detector electronics with this frequency. Even after imposing zero suppression, which largely reduces amount of data coming from the experiment it would not be possible to read and store data for all collisions. The maximum rate of events which can be stored on disk is about 10-15 Hz. It is the main role of the Trigger system to recognize interesting events, which should be stored and reject other events in particular those not resulting from electron-proton collision. When running with high luminosity also many events resulting from electron-proton collisions are not useful for analysis and Trigger System is also supposed to reject such events.

The Trigger System of ZEUS experiment consists of three levels with the output trigger rate of 1 kHz, 100 Hz and 10 Hz, for the First Level Trigger (FLT) [14], the Second Level Trigger (SLT) [15] and the Third Level Trigger (TLT) [16], respectively. In order to keep deadtime on acceptable level (less than 5 %) data coming from the detector are stored in electronic pipelines (FLT level) or buffered (SLT and TLT) while the trigger decision is being processed. After positive decision at each trigger level, raw event data from all components are stored to mass storage system (disk and tapes in DESY Computer Center) for further processing. Before they can be used for physics analysis dedicated code is used to apply calibration and alignment corrections and to reconstruct variables describing global event properties. In this chapter trigger and data acquisition system elements are described. The general scheme of the ZEUS trigger and data acquisition system is presented in Figure 4.1.
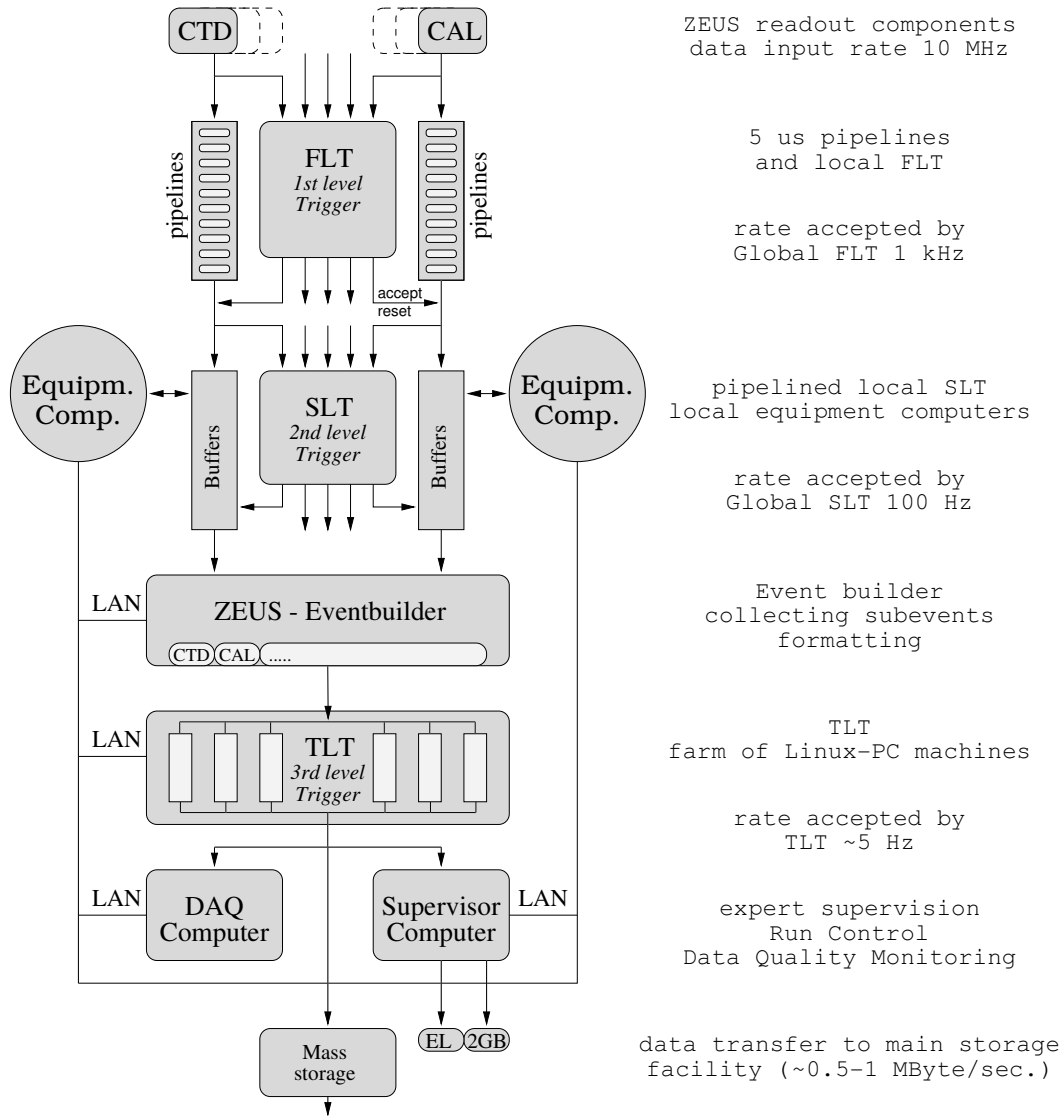
Figure 4.1: Scheme of the ZEUS trigger and data acquisition system
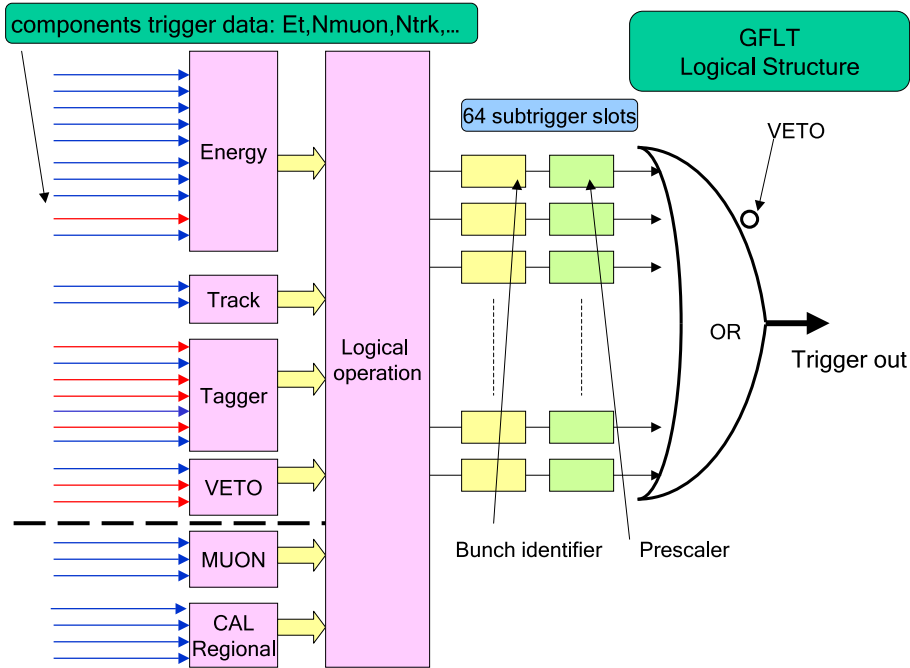
Figure 4.2: Scheme of the GFLT logical structure.

4.1   First Level Trigger

The design of the ZEUS trigger system assumes that various components read signals from front-end electronics and store their data into digital or analog pipelines with HERA 10MHz clock. Simultaneously, subsets of the data referring to the same bunch crossing are analyzed by local first level triggers of the components (see eg. [17]) and the resulting trigger variables are sent to Global First Level Trigger (GFLT) [14] within 2.5 μs. The scheme of the GFLT logical structure is shown in Figure 4.2. The component trigger data available at the GFLT include following variables from main detector components:

- total transverse energy (E_t) and missing transverse energy ($E_t^{missing}$) from CAL,

- number of tracks (N_{trk}) from CTD,

- primary and secondary vertex positions from CTD and MVD,

- numbers of muons identified in FMUON, BRMUON and BAC.

Figure 4.3: The First Level Trigger (GFLT) trigger board.
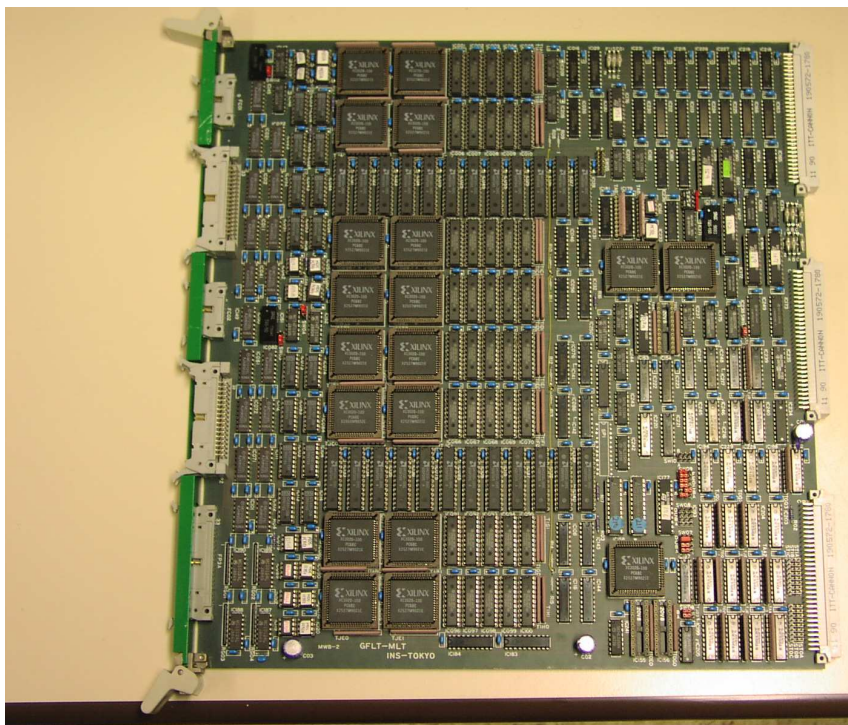
GFLT consists of a set of dedicated, programmable electronic boards (see Figure 4.3). On the GFLT level trigger data from different components are matched and compared with predefined criteria. Data processing at GFLT is performed on the hardware level using programmable lookup tables memory (LTM). This allows for very fast computation of the final decision. The main role of the GFLT is to reduce up to about 1 kHz accepted events rate. Within 4.4 μs after bunch crossing the GFLT decision is taken, negative or positive. If negative decision is taken no further action is required. If the trigger data fulfill one of the trigger logic conditions a positive decision so called "accept" is distributed to all components of the ZEUS experiment. Receiving GFLT "accept" components are requested to copy event data from pipelines to memory buffers and proceed to the second step of the event selection algorithm.

To reduce rate of events processed on the SLT level, the so called "fast clear" mechanizm was implemented. More detailed information from CAL is processed and, if the CAL FLT decision is not confirmed, "fast clear" signal is sent to all components to abort processing of the "accept" decision.

4.2 Second Level Trigger

Contrary to GFLT, where data processing is strongly limited by timing con-
strains, more time available at the Second Level Trigger (about 8 ms) allows
us to perform much more complex data analysis. The SLT algorithm is
implemented in a code running on a network of parallel microprocessors -
INMOS T800 Transputers [18]. After the GFLT "accept", the data from
all detector components are read out and stored in the second level trigger
buffer. Simultaneously, subset of the data extracted by the component SLT
algorithm is analyzed and passed through the SLT network to the Global
Second Level Trigger (GSLT) [15].

All trigger variables available at GFLT are accessible at the SLT as well.
In addition new variables are calculated at the SLT level including CAL
timing, list of electron candidates, reconstructed hadronic clusters and muon
candidates. The Calorimeter timing is very useful in rejecting background
events not coming from ep collision. For particles produced in ep collisions,
calorimeter response time corrected for the distance between the given CAL
cell and IP should be consistent with 0. For beam related backgrounds
time shift is expected as particles are produced far from nominal IP. For
backgrounds not related to the beam, dominated by cosmics, CAL timing is
uniformly distributed over 96 ns window and the shift between timing in the
upper part and lower part of the detector is expected.

Similar to GFLT, the GSLT combines trigger information from various
components and produces 32 subtrigger bits, each corresponding to one pre-
defined event selection criteria. If at least one of 32 subtriggers fulfills the
corresponding condition, the GSLT accepts the event and the positive deci-
sion is distributed to all components of the ZEUS experiment. The GSLT
reduces the event rate down to 100 Hz.

4.3 Event Builder and Third Level Trigger

The main task of the Event Builder [19] is to collect data coming from com-
ponents and to build the final data structures consistent with the ADAMO
[20] data base records used for finale storage. After the positive GSLT de-
cision, component data corresponding to this decision are collected and the
event is passed to the Third Level Trigger (TLT) [16] for further analysis.

The TLT implementation is based on the farm of linux PC machines
running simplified version of the off-line reconstruction software. Similar to
GFLT and GSLT, TLT output is given as a set of subtrigger bits, each bit
corresponding to a specific selection criteria prepared by the physics analysis

groups. The selection algorithms, so called "physics filters" are based on quantities such as scattered electron energy and angle, jet energies, invariant mass of the produced final state.

At the TLT level, it is possible to classify and select events according to physical processes that occurred at the IP. An event is accepted if it passes one or more of the TLT "physics filters". Accepted events are transfered to the DESY Computer Center and recorded on tape. The design of TLT allows to reduce the event rate up down 10 Hz.

4.4   Run Control

In order to synchronize trigger processing and data flow of all components the dedicated Run Control (RC) system has been implemented [21]. The main goal of the Run Control is to establish communication between the central trigger components (GFLT, GSLT, EVB, TLT) and all detectors through a Local Area Network. The Run Control distributes commands to all components i.e to all detector readout systems and to central trigger components. The following commands are used to collect data from the experiment:

- SETUP: setups all components and prepares for data taking,

- ACTIVATE: starts the data taking of the experiment,

- END: finishes data taking,

- ABORT: stops the data taking, used in case of system problems,

- SKIP: skips execution of previously issued commands.

In reply to the commands sent Run Control receives status information from components. It also receives error messages, giving opportunity to check consistency of the data flow. In addition, dedicated monitoring tasks collect selected data from components allowing for instant check of data quality (so called Data Quality Monitoring, DQM).

4.5   Event Reconstruction

As mentioned above, events accepted by the Third Level Trigger are stored to the mass storage system. For reconstruction of the collected data a dedicated program ZEPHYR has been developed (Zeus Event Physics Reconstruction).

The data reconstruction and analysis can be divided in few "phases". In the first phase calibration corrections are applied to the data. Dead and noisy channels are removed. Reconstruction codes specific for each readout component (track reconstruction in CTD, cluster reconstruction in CAL, muon reconstruction in BMUON, FMUON and BAC) are also run.

In the second reconstruction phase, information from various components is combined to obtain more global quantities as missing transverse momentum or list of electron candidates (combining information from CAL and tracking detectors).

The final phase of ZEPHYR includes running algorithms that define the "physics filters". The definition of the filters allow to select the specific physics process (e.q J/Ψ production or NC DIS). In general, same physics filters are used as on TLT level, but some of the selection criteria are stronger (TLT level cuts can not be made too restrictive as detailed calibration information is not available).

For events passing at least one physics filter, output of the ZEPHYR reconstruction is stored into the Data Summary Tapes (DST). Information about the decision of the physics filter algorithms is included as the so called DST bits. In addition, the DST bits are stored in a separate file, to allow for more efficient event selection in further analysis.

4.6   Data Analysis

In order to perform physics analysis the individual user can access the reconstructed event data, including reconstructed component and global quantities, via EAZE and ORANGE programs. These software frameworks allow to implement dedicated data processing code (in FORTRAN or C) that imposes non-standard event selection criteria and calculates additional physics quantities and other variables needed for the analysis. Output of the EAZE and ORANGE programs, which are processed on the DESY computer farm, can be further analyzed with graphical analysis tools PAW and ROOT. An overview of the physics analysis environment of the ZEUS experiment can be found in [22].

4.7   Monte Carlo Simulation

All physics analysis of the ZEUS data is based on the comparison of the measured event distributions with model predictions, as obtained from the detailed Monte Carlo simulation of the experiment. Simulation of the physics

processes performed by using ZDIS package which allow to steer a number of MC generators. The output is then passed to the ZEUS detector simulation program MOZART (Monte Carlo for ZEUS Analysis Reconstruction and Trigger). This program is based on the CERN GEANT 3.13 package [23]. The trigger chain simulation is done by the dedicated program ZGANA. Finally simulated event sample is reconstructed using ZEPHYR and stored in ADAMO format consistent with the one used for real data. With this procedure the individual user can use the same code to analyze both the data and simulation samples.

Chapter 5

The Backing Calorimeter

5.1   Mechanical Construction

The Backing Calorimeter design is based on the iron plates of the detector yoke and aluminum proportional chambers. Schematic view of the Backing Calorimeter is presented in Figure 5.1. The ZEUS detector is asymmetric and so is the iron yoke, used as the absorber for the BAC. In the central part the yoke is made out of 10 iron plates, whereas in forward and rear it consists of 11 and 8 plates respectively. Therefore the forward part of BAC (Forecap) is equipped with 10 layers, the central with 9 and Rearcap with 7 layers of the chambers. From the point of view of mechanical structure the central part of BAC is divided into two parts: lowest, horizontal part of yoke, being a support for all central components of the ZEUS detector is referred to as Bottom and the rest of central part of yoke, which can be moved apart, is called Barrel.

The aluminum proportional chambers of the Backing Calorimeter are typically 5 m (Endcaps, Barrel) and 7.5 m (Bottom) in length and are inserted in the gaps between iron plates used as a calorimeter absorber material. The BAC detector was constructed using about 5200 chambers, covering in total the surface of 3500 m^2. From mechanical and readout point of view BAC is divided into 13 "areas". Eight areas in Barrel are defined by dividing it according to the chamber location: forward or rear, north or south and up or down. Forecap and Rearcap are divided into two areas each, corresponding to north and south parts of endcaps (see Figure 5.1). Finally, Bottom is considered as a separate area.

Sense wire direction in all chambers is horizontal. Wires are parallel to the axis of HERA beams in the Barrel and Bottom parts of the detector and perpendicular to this axis (i.e along X axis) in Endcaps. A single cham-
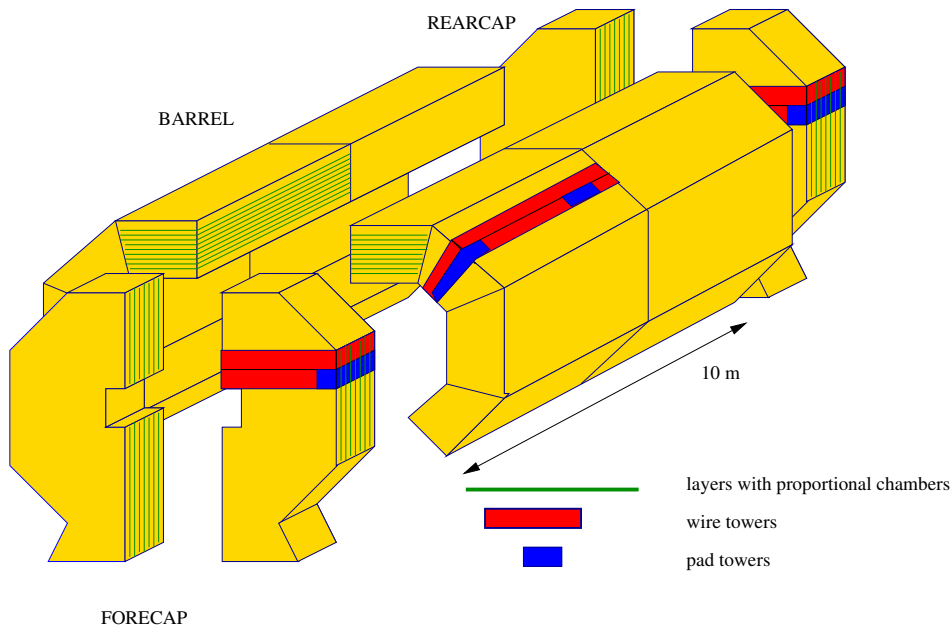
Figure 5.1: Schematic view of the Backing Calorimeter, with indicated division into Forecap, Barrel and Rearcap and the location of the energy readout towers (the Bottom in not presented on this picture).

ber consists of 7 or 8 cells (see Figure 5.2) with transverse dimensions of 15x11 mm^2 each. Anode wires with 50 μm diameter are stretched along the centre of each cell. Aluminum cathode pads (each 50cm long) cover all cells from the top. Gas mixture of 87% Ar and 13% CO_2 is filling the chamber at the pressure close to the atmospheric one.

5.2   Readout Structure

Aluminum proportional chambers are the active element of BAC and the source of all measured signals. Charged particles passing through the chamber ionize the gas mixture. Due to the electric field produced by the high voltage[1] applied between the anode wire and cell walls (cathode), electrons move in the anode wire direction, while positive ions drift towards the cathode. In the region of very high electric field, close to the thin anode wire, electron scattering can result in secondary ionization leading to the so called "gas amplification" phenomena. The charge which is finally collected on the

---

[1]High voltage of 1785 V was used until 2005. After full implementation of the BAC muon trigger high voltage was raised to 1800 V to improve position readout and trigger efficiencies.
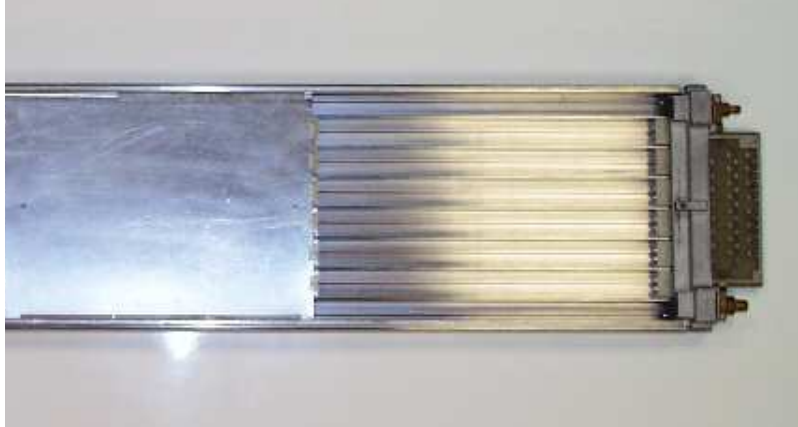
Figure 5.2: The view of the BAC aluminum proportional chamber. To show the cell structure the cover and a part of one cathode pad was removed.

anode wire is few orders of magnitude larger then the primary ionization, but is proportional to it (the chamber working in this regime is called a proportional counter).

The Backing Calorimeter readout can be divided into two parts: an energy and a position ones. In the energy readout (also referred to as an analog readout) signals from individual chambers are summed over a larger number of chambers in a layer and over all detector layers, corresponding to a geometrical region called a "tower" (see Figure 5.1). In the position readout (also referred to as digital or hit readout) each individual anode wire is read out, it's signal compared with a predefined threshold and binary result of this comparison stored in a pipeline. The readout process runs continuously with HERA 10 MHz clock. The total number of position readout channels (number of wires in all chambers) amounts to about 40000, while the number of analog channels is about 2000.

Hit Readout

The position readout enables us to reconstruct tracks of particles in the plane transverse to the wire direction. Toroid magnetic field, which is produced in the iron yoke by dedicated magnets is perpendicular to the readout wire direction in Barrel. Charged particle tracks bend in the plane parallel to the wire, so the track curvature is not measured in the BAC position readout and only stright particle tracks are expected.

In order to handle the digital wire readout dedicated electronics called "hitbox" was installed. The role of hitboxes is twofold: they store the data read from all wires for the time needed to develop GFLT and GSLT decisions

and calculate the trigger variables for BAC First Level Trigger.

The hitbox is directly connected to the anode wire readout electronics. The signal is sent to the discriminator circuits and the binary information from comparing the signal to a predefined threshold is stored into 6 μs (64 HERA clocks) pipelines. One 8 bits word stored in a pipeline corresponds to pattern of wires "hit" by particles in single chamber. In case of the positive GFLT decision readout hardware reads the data from pipelines and stores them to the second level trigger memory (Dual Port Memory - DPM) also located in the hitbox (on the so called buffer board). In order to reduce the data volume a zero suppression mechanism was implemented, rejecting empty hit patterns.

While the binary data are being stored in the pipeline, the hitbox calculates also the corresponding trigger variables and transfers them to the higher level of BAC FLT for further processing. This part will be described in details in the second part of this chapter.

Analog Readout

In the analog wire readout, the wire signals from three or four neighboring chambers are summed over all calorimeter layers. Such a structure is called a "wire tower" (see Figure 5.1). Schematic view of the analog wire readout is presented in Figure 5.3. The total charge collected from a wire tower is transfered to the so called "shaper", where it's converted to the voltage pulses with uniform shape. After "shaping" the pulse is forwarded to FADC (Fast Analog to Digital Converter) sampling the pulse with 10 MHz clock. To increase the dynamical range of the readout (FADC is 8 bit only) the signal of each wire tower is split into two channels, one of which is amplified by an additional factor of about 6. The wire towers amount to 356 readout channels.

In order to achieve better spatial granularity of the energy measurement a pad readout was implemented. The pad signal from three or four adjacent chambers is summed over all calorimeter layers forming the so called "pad tower" (see Figure 5.1). The typical transverse dimension of such a tower is 50x50 cm^2 providing a sufficient accuracy to match with the position of a hadronic shower measured in CAL. In addition, the pad readout allows us to estimate the position along the wire direction for muons identified in the hit readout. The signal from a pad tower is shaped and transfered to FADC, as it is done for wire towers. The pad towers amount to 1692 readout channels.

For the trigger purpose the Backing Calorimeter was also equipped with the so called strip readout. The single "strip tower" consists of a sequence of neighboring pad towers located at the same polar angle w.r.t the center of
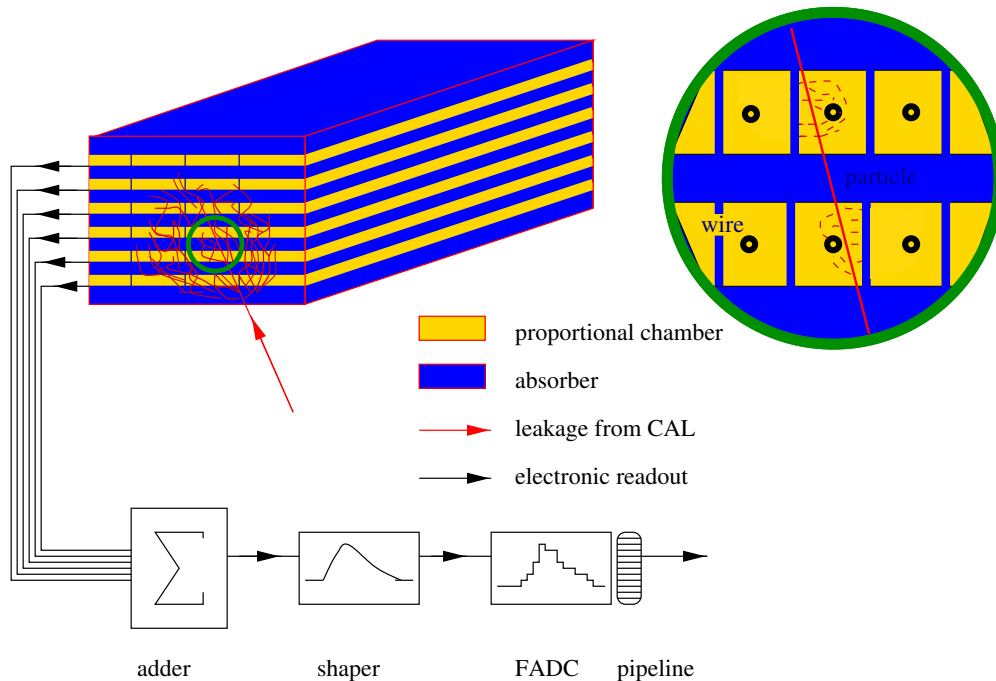
Figure 5.3: Schematic view of single analog wire tower (with possible development of the hadron cascade) and the the electronic chain of the readout

the ZEUS detector (nominal IP). The strip towers are used to calculate the transverse energy (E_t) one FLT and SLT levels. The strip towers amount to 133 readout channels.

5.3 Data Acquisition

Collecting the data from the BAC and combining BAC data with data from other ZEUS components would not be possible without the dedicated data acquisition system (DAQ) [21]. BAC DAQ consists of two parts: control system running on VMS workstation (so called equipment computer - EQC) and distributed DAQ running on the transputer network. The role of the data acquisition is the following:

- Handling the First Level Trigger

  The GFLT decisions are continuously distributed to all components. The rate of accepted events is up to 1kHz corresponding to time interval of 1ms between consecutive events. After the positive GFLT decision the DAQ system reads the corresponding subset of data from memory,

   calculates the BAC SLT variables and sends results to GSLT within
   4 ms. Consecutive events are processed in parallel.

- Handling the Second Level Trigger and preparing data for Event Builder

   In case of the positive GSLT decision, the DAQ system reads the data
   referring to the given of GSLT decision and packs them in structures
   readable for Event Builder. As soon as the packing procedure is fin-
   ished, the DAQ sends the data to the Event Builder (EVB).

- Control and Synchronization with Experiment

   In order to synchronize and control the process of data acquisition by
   different components the ZEUS experiment is equipped with the central
   Run Control (see Section 4.4). As it is the case for all components,
   the data acquisition system of the BAC receives commands from Run
   Control and proceeds accordingly. For each command received by the
   BAC control system, a command or a series of commands is distributed
   to the BAC transputer network.

The design of the Data Acquisition has been implemented almost 15 years
ago, in 1991. Meanwhile, several reconfigurations have taken place following
the development of the ZEUS experiment. As one of the major upgrades, was
related to the implementation of the BAC muon trigger system after HERA
upgrade in 2000-2002. The Data Acquisition software has been written in
OCCAM 2 under Alpha-station/VMS. The main attribute of this software is
its modularity that maps very well on transputer network. Control system
and user interface have been writtten in Fortran and C.

Readout Hardware

The total number of readout channels of the Backing Calorimeter is about
42,000 (40,000 digital and 2000 analog channels). The readout electronics
have been grouped in three different locations: on the so called "balconies"
at the base of the ZEUS detector on the north and south sides, and in the
rucksack. The cable length between the balconies and the rucksack is about
60 meters.

The readout boards are placed in 19 VME crates. The device controlling
each VME crate, so called crate master is a 2TP-VME board designed by
NIKHEF. The board consists of two INMOS T800 Transputers [18] (called
TPx and TPy) with 4MB memory each and 128kB triple-port memory
(TPM). The 2TP-VME boards include also the full VME interface [25].

The data acquisition system is controlled by the BAC equipment computer (EQC). EQC (Alpha-station with VMS operation system) communicates with the transputer network trough a CAPLIN Cybernetics QT0 link interface. CAPLIN interface is connected with the transputer network via the optical fiber link. EQC is used to boot the transputer network and to synchronize the readout task with the rest of experiment.

Transputer Network Structure

The main role of the DAQ system is to prepare BAC SLT data for GSLT (in response to GFLT "accept") and to send collected BAC data to EVB in case of positive GSLT decision. These two main goals of BAC DAQ are reflected in the structure of the transputer network, which can be divided into SLT and EVB subnetworks. It was decided that in each network node transputer TPx belongs to SLT subnetwork, while TPy to EVB one. As a fast and convenient way of data transfer between both transputers, the TPM is used. In case of accepted GFLT event, the TPy processor reads the subset of data from readout board memory buffers (via VME bus), copies it to the TPM and sets interrupt to TPx. In response to the interrupt TPx processor reads the data needed by the BAC SLT algorithm from the TPM and starts calculating SLT variables.

In case of positive GSLT decision TPy processor reads all data stored in readout memory buffers, converts the data to the ADAMO format and transmits it to the EVB via EVB subnetwork. The EVB subnetwork was designed as a binary tree. The advantage of this solution over a standard linear daisy chain is that the maximum path length grows as $\log(N)$ instead of N, where N is the number of transputer nodes.

For communication with the central components of the experiment the Data Acquisition has been equipped with external interfaces to: Global Second Level Trigger (GSLT), Event Builder (EVB) and Equipment Computer (EQC). The communication with GSLT and EVB is based on a standard transputer links.

Communication with GFLT

Following the ZEUS Global First Level Trigger design, the Backing Calorimeter is equipped with a dedicated electronics which is responsible for communication with GFLT and distribution of GFLT decisions to the readout boards. To assure proper distribution of GFLT decisions and to synchronize the readout electronics with the GFLT a dedicated BAC First Level Trigger

(BFLT) protocol was implemented [24]. The BFLT electronics consists of the followings boards:

- Global First Level Trigger Board Interface (GFLTBI)

  The board is responsible for handling the GFLT protocol signals and for generating the BAC First Level Trigger protocol signals distributed to other BFLT boards.

- Scanners

  Boards which control data collection from the analog readout (wire, pad and strip towers).

- Distributors

  Boards which control the position readout (hit-boxes).

The BFLT protocol defines timing dependencies between the following signals:

- CLOCK - HERA clock signal used to synchronize readout electronics,

- ACCEPT - signal corresponding to positive GFLT decision,

- BUSY - signal indicating an event reading in the readout electronics is in progress,

- ABORT - request for event reading abort.

Handling of the GFLT decisions will be described in more details in chapter 7.

5.4   BAC FLT

BAC First Level Trigger [13] was designed to recognize events with significant energy leakage out of the central uranium calorimeter and to identify muons produced at the interaction point. Due to strong time limitations the algorithm had to be implemented on the hardware level using dedicated circuits. From geometrical point of view, as described in section 5.1, BAC can be divided into 13 areas: 8 in Barrel, 4 in Endcaps (Forecap and Rearcap) and Bottom. This division is also reflected in the design of the BAC FLT. The single area is the smallest unit of the BAC detector for which the trigger variables are calculated

BAC FLT consists of two independent trigger branches: an energy and muon triggers. Following trigger variables are calculated for each area: energy, transverse energy and 4 bits of muon identification. Decision variables calculated on the area level are then combined to determine global BAC FLT variables: the values of total energy and total transverse energy measured in BAC (both calculated with 16 bit precision), values of two highest energy deposits with their location and 15 bits of muon information. The final BAC FLT data is calculated within 2.5 μs after *ep* collision, corresponding to 26 HERA clocks. After this time BAC FLT variables are transferred to the Global First Level Trigger. The GFLT gathers and combines data from different components. If the event is interesting from the analysis point of view, a positive GFLT decision is distributed to all components of the ZEUS experiment.

BAC muon trigger implementation and its performance are the main subjects of this thesis. In the following design of the BAC First Level Trigger is described in details.

Structure of the Energy Trigger

The structure of the BAC FLT energy trigger is illustrated in Figure 5.4. The energy trigger decision is based on the data coming from the wire and strips towers. Signals from wire towers are processed by WTT (Wire Tower Trigger) boards, while signals from strip towers are processed by STT (Strip Tower Trigger) boards. Analogue signals corresponding to the measured energy deposits are first digitized by 8-bit FADCs. After conversion the data are stored into pipelines. Simultaneously the data are fed to a so called Local Maximum Finder (LMAXFI). This circuit looks for the local maximum in the input data stream according to the condition:

$$A_{in}(i-1) < A_{in}(i) \geq A_{in}(i+1) \tag{5.1}$$

where: A_{in} is the amplitude of incoming signal, while $(i-1)$, (i) and $(i+1)$ denote the consecutive FADC samplings.

When the local maximum is detected its value is returned for two subsequent clock cycles, otherwise null value is returned. The maximum detected by LMAXFI becomes the reference address for the programmable memory array (LTM, look-up table memory). This solution allows to perform fast operations on data in one clock cycle.

The WTT board contains one LTM for each input channel. LTM is addressed by 8 bits corresponding to the measured energy deposit and Y bit coming from the position readout (see following subsection). The extra Y
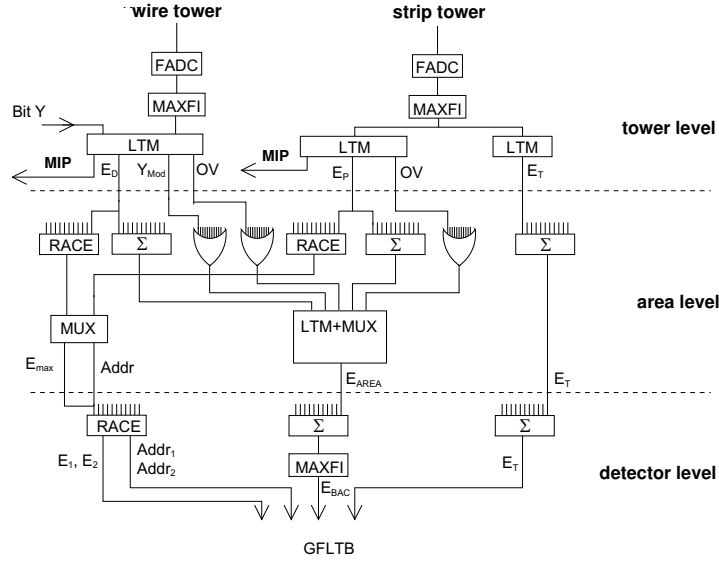
Figure 5.4: Detailed structure of the BAC FLT energy trigger.

bit enables us to veto deposits that have not been confirmed by the position readout. The LTM implemented on the WTT board has 11 bit output, 8 of which are used to code the calibrated energy, while the remaining 3 are used as binary flags indicating: minimum ionization particle (MIP), FADC overflow or the deposit that hasn't been confirmed by position readout.

The STT boards contain two LTMs for each input channel. One is used for energy and the other one for the transverse energy measurement. Both LTMs are addressed with 8 bits of the measured energy value. The memory used for determination of the transverse energy on the STT board has an 8 bit output. The LTM used for energy determination has a 10 bit output, where 8 bits correspond to calibrated energy and the remaining two bits are flags indicating minimum ionizing particle (MIP) and FADC overflow. On the STT and WTT boards, the sum of energy and transverse energy over the whole area is also calculated. Bits corresponding to minimum ionizing particles are counted. The highest energy deposit together with its location is also determined, separately for wire and strip towers. All these values are transferred to the main trigger board of the area called LT (Logic Trigger) for further processing.

Structure of the Muon Trigger

The BAC muon trigger decision is based on the data from the position readout. For each wire tower the dedicated circuit calculates two quantities: the
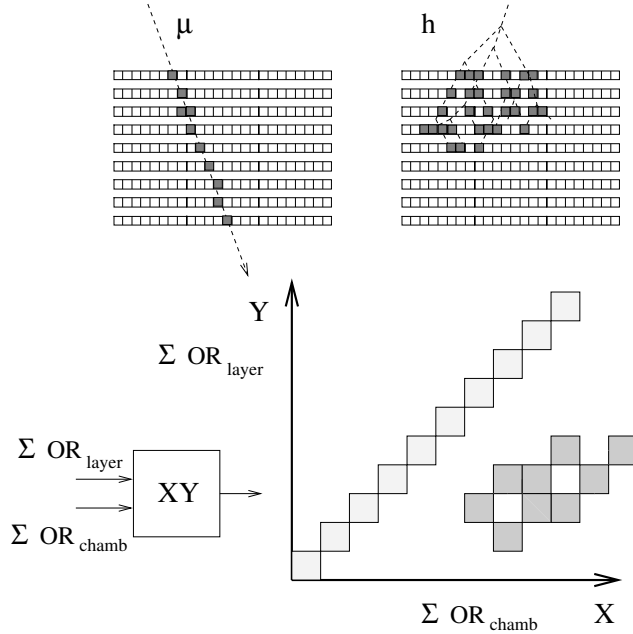
Figure 5.5: The idea of the BAC muon trigger algorithm.

number of "active" layers and the number of "active" chambers. The layers is "active" if at least one chamber has been hit by the particles. The chamber is "active" if at least one wire has been hit. Position readout of each wire tower is equipped with LTM which allows to separate muon from hadron cascade using fast pattern recognition. This LTM has 10 bit input (address space): 6 bits correspond to the number of "active" chambers and remaining 4 bits correspond to the number of "active" layers. Output of this memory has only 2 bits marked as X and Y.

The algorithm separating muons from hadron cascade (pattern recognition) is the following: if the number of "active" layers is approximately equal to the number of "active" chambers then this event is consistent with the observation of a minimum ionizing particle, that is a muon. In this case bit X is set to 1 (see Figure 5.5). Otherwise, when the number of "active" chambers distinctly exceeds the number of "active" layers, such an event corresponds to an observation of the hadron cascade and Y bit is set to 1. When the number of "active" layers and "active" chambers is very low such an event is treated as noise or empty event and bits X and Y are set to 0.

One area contains from 10 up to 16 wires towers for which X and Y bits are calculated. These bits are transferred to the XYREC board (see Figure 5.6) for the further processing. The basic function performed by this board is synchronization of X and Y bits (coming from different towers), masking of

Figure 5.6: The "XYREC" trigger board

faulty channels and performing the sum of X bits. Y bits are being forwarded
to WTT boards, while the sum of the X bits to the LT board.

Processing of Data from Area

Processing of data from area is performed at the LT (Logic Trigger) boards
and is also based on look-up table memories (LTM). The LT board contains
two LTMs, one of which is used for processing the energy data, and the other
one to classify muons according to the topology of their trajectory.

The final energy from the area is calculated using multiplexing circuit
(MUX), which allows to choose between the deposits measured in the wire
and in the strip towers. The algorithm takes into account the energy correc-
tions, overflow bits and bits indicating the response of the position readout.
In this way it is possible to choose the more credible energy deposit value,
i.e. the value which is less biased.

To classify muons, the LT board uses the arithmetic sum of the X bits
coming from the XYREC board and the number of MIPs from WTT and STT

boards. The algorithm to classify muons is based on the following principle: muons coming from random directions usually cross a large number of towers, whereas muons produced at the interaction point cross only 1 or 2 towers. Based on the information from both the position and the energy readouts, muons are classified as those produced at the interaction point, cosmic muons and the muons which can be used for calibration (mostly beam-halo muons).

The LT board produces the following trigger variables for each area: 12 bits for the energy, 12 bits for the transverse energy, the highest energy deposit together with its location and 4 bits of muon identification.

Processing of Intermediate Data

The BAC trigger electronics components have been grouped in three locations: in the north part of the detector (north balcony), in the south part (south balcony) and in the rucksack. At each balcony E, Et and the muon identification bits from 6 areas are determined. Calculation of the total energy and the total transverse energy is performed at two identical boards, called ADDER. The task of finding two highest deposits together with their locations is performed on the so called RACE board. Determination of the muon identification bits is performed by the so called BITS boards. The output variables from BITS boards contain information about the muon classification from 6 north and 6 south areas. All boards mentioned above are also responsible for synchronizing the signals received from different areas.

The data from Bottom are not included in this processing stage, as they are processed by electronics located in the rucksack. Trigger information from Bottom is combined with that from other areas only at the final stage.

Final Trigger Data

The algorithms used to calculate final trigger variables are implemented on the so called MAIN boards: EMBAC, RMBAC and BMBAC. The EMBAC board calculates the total energy and the total transverse energy measured in BAC. Two highest energy deposits with their physical location are determined by the RMBAC board. The BMBAC board returns 15 bits of the muon identification based on the input from the BAC position readout: 13 bits contain information about muons from interaction point at individual areas and 2 additional bits code the information about cosmic and calibration muons. The final output of the BAC FLT, as sent to GFLT, consists of 77 bits of trigger data: 16 bits of energy, 16 bits of transverse energy, the value and physical location on the detector of the two highest energy deposits and 15 bits muon identification.

In addition to the nominal operation mode described above (designed for ZEUS data taking), the BAC can also operate in the so called "local mode" sending the final BAC FLT variables to the local trigger board. This mode of operation is used to test the performance of the trigger without the necessity of including BAC into the full DAQ chain of the ZEUS experiment.

Chapter 6

Trigger Setup and Optimization

The Backing Calorimeter muon trigger design is based on many different hardware components, as described in the previous chapter. Most of the readout and trigger boards involve programmable circuits and LTMs. Moreover, trigger processing and data acquisition is controlled by software running on the transputer network. The degree of complexity of this system is such that the startup and optimization procedure had to be performed in many steps. Author of this thesis was involved in all stages of Backing Calorimeter electronics tests and was one of the persons responsible for the trigger startup and optimization. In the following sections subsequent phases of the trigger startup are described.

6.1 Trigger Electronics Tests

In order to startup the trigger electronics and to achieve optimum performance of the trigger system, dedicated diagnostic software has been developed. The kernel of this diagnostic system consists of a package written in OCCAM-2 language which implements VME-BUS read and write cycles and includes also a set of control functions specific to the readout and trigger electronics of the Backing Calorimeter. Most of tests benefit from the fact that the trigger electronics is equipped with internal diagnostic modules which enable various tests and checking [26]. In addition, most of the trigger electronics include very flexible Field-Programmable Gated Array (FPGA) chips from ALTERA, which allow us to perform extended hardware diagnostics and debugging of the whole trigger chain. Many of these "ALTERAs" boards were designed and built as a completely new and unique hardware, dedicated for BAC upgrade. Therefor detailed tests of these boards were performed in our lab even before they were installed in the VME crates at

the experiment. At this stage, many modifications of the dedicated ALTERA code (prepared in VHDL language) had to be performed to obtain optimal board performance. After multiple tests, the final version of ALTERA code (so called "bootfiles"), to be used in the experiment, was established.

In addition to the diagnostic system, a dedicated database has also been developed to collect data from complex tests of the whole system, as installed at the ZEUS experiment. The database also contains the information about the detector geometry, location of electronics crates and boards, cabling and mapping of the readout channels onto the detector structure. Results stored in the database allow us to prepare an optimal detector and trigger setup for data taking. These results are also very valuable for the Monte Carlo studies, because they allow us to reproduce the actual detector running conditions in simulation.

From the point of view of the trigger system design, trigger electronics tests can be divided into the following categories: software functional tests, trigger integrity tests and system performance tests.

Software Functional tests

Software functional tests are mainly intended to recognize and mask out faulty electronic channels. As mentioned above, BAC readout and trigger electronics is equipped with many different pipelines, buffers, counters, control registers and LTMs. Many of these "memory locations" can be directly accessed using dedicated electronics and software tools. As an example, the idea, implementation and results of the "hitbox" front-end electronics tests are presented below.

The idea of tests is based on the following principle. Accessible "memory locations" are filled with predefined data pattern consistent with their data structure. In order to verify the hardware performance, the data are read out from these locations and compared with test pattern. Varying data patterns are used, to be sensitive to all hardware problems (missing bits, noisy bits, address errors etc.) In case of any inconsistency, corresponding hitbox is marked as broken and detailed test results are stored in the database. Shown in Figure 6.1 is the information stored in the database after hitbox electronics tests and threshold trimming (described in the later part of this chapter). Marked in red are BAC chambers for which hit readout failed to pass the tests.

Unfortunately the hitbox electronics turned out not to be very reliable. Functional electronics tests had to be repeated few times a week. Failure of a new hitbox was detected approximately once a week. As the ZEUS detector (and so the Backing Calorimeter) was regularly serviced (at least
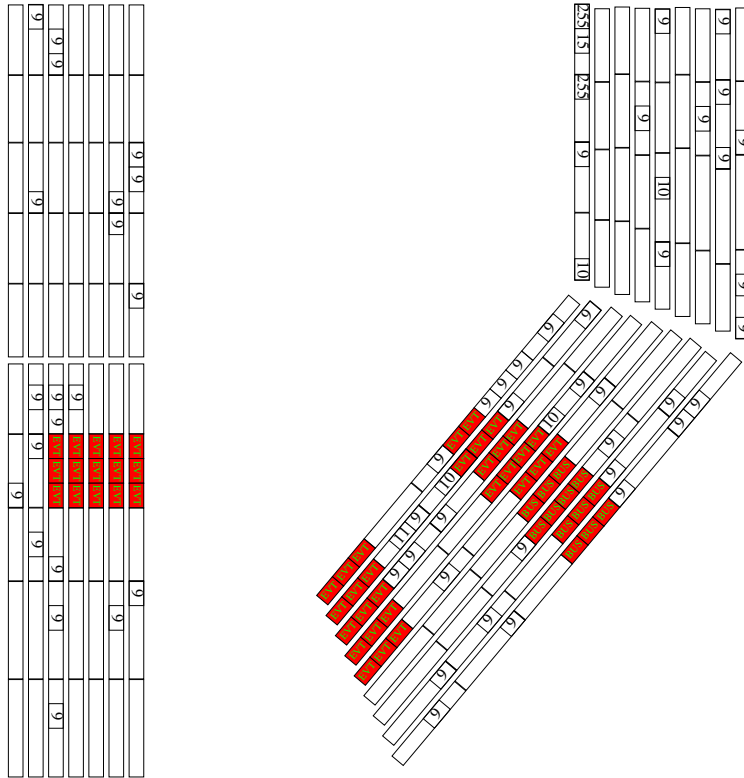
Figure 6.1: Results of the hitbox electronics tests and threshold trimming, as stored in test result database (only part of the detector is shown).

once a month, during the so called monthly access), we were able to keep the average number of broken hitboxes at the level of about of 10 % (35 out of 356).

Trigger Integrity Tests

Trigger integrity tests are used to trace the whole trigger and data acquisition chain with various trigger settings. In addition, these tests were also intended to verify reliability of trigger boards for which VME-BUS write-read cycle cannot be applied (STT, WTT and LT boards) . The idea of tests is the following: trigger configuration and readout is set as for normal data taking and the full data acquisition is run, but with extended diagnostic. However, BAC is running in the "stand-alone" mode, without involving other components of the ZEUS experiment. Instead of reading signals from BAC chambers, pipelines are filled with test patterns. The GFLT signals are simulated at BAC GFLT interface board (GFLTBI) and the collected data are directed

to BAC EQC. When trigger protocol error or trigger data inconsistency is detected, corresponding message is written in the logfile and stored in the database. Integrity tests allowed us to detect and correct following types of hardware malfunctions: dead channels, communication problems, signal polarization inversion, bit swapping (from improper cabling), trigger algorithm malfunction.

Trigger Performance tests

Trigger performance tests are done with use of analog test pulses or with cosmic ray data. The analog pulse can be injected into selected preamplifier or a group of preamplifiers and used to simulate the detector data (so called charge injection). As for cosmic rays, taking into account that the ZEUS detector is located in an experimental hall below the ground level, covered with a concrete shielding and that the BAC trigger tower surface is about 2.5 m^2, cosmic trigger rate of the order of 10 to 100 Hz is expected from single trigger tower (depending on the position in the detector). Trigger Performance tests check the full performance of the detector and trigger. Both for charge injection and for cosmic ray tests, trigger electronics processes true data coming from the detector.

The idea of the performance test is the following: the system is set up and full data acquisition is run. In addition to the standard data stream, dedicated diagnostic modules of the trigger electronics allow us to fill trigger rate histograms with 10MHz HERA clock. Example trigger rates observed in cosmic test run are shown in Figure 6.2. Each of the 13 plots shows the average cosmic trigger rates for wire towers within one area. Highest rates are observed in areas 4 to 7 (plots in the central column of Figure 6.2), which correspond to the upper part of Barrel. Gaps observed in the rate distribution correspond to channels which are not used (e.g. all "down" areas are only equiped with 10 trigger towers, see left column in Figure 6.2) or to faulty trigger channels.

6.2   Threshold Trimming

To obtain best possible separation of the real particle signal from the chamber or electronic noise hit readout discriminator thresholds should be adjusted separately for each individual channel. For that purpose a dedicated threshold trimming procedure has been developed. In order to reproduce detector running conditions during the threshold trimming procedure the following criteria need to be fulfilled:
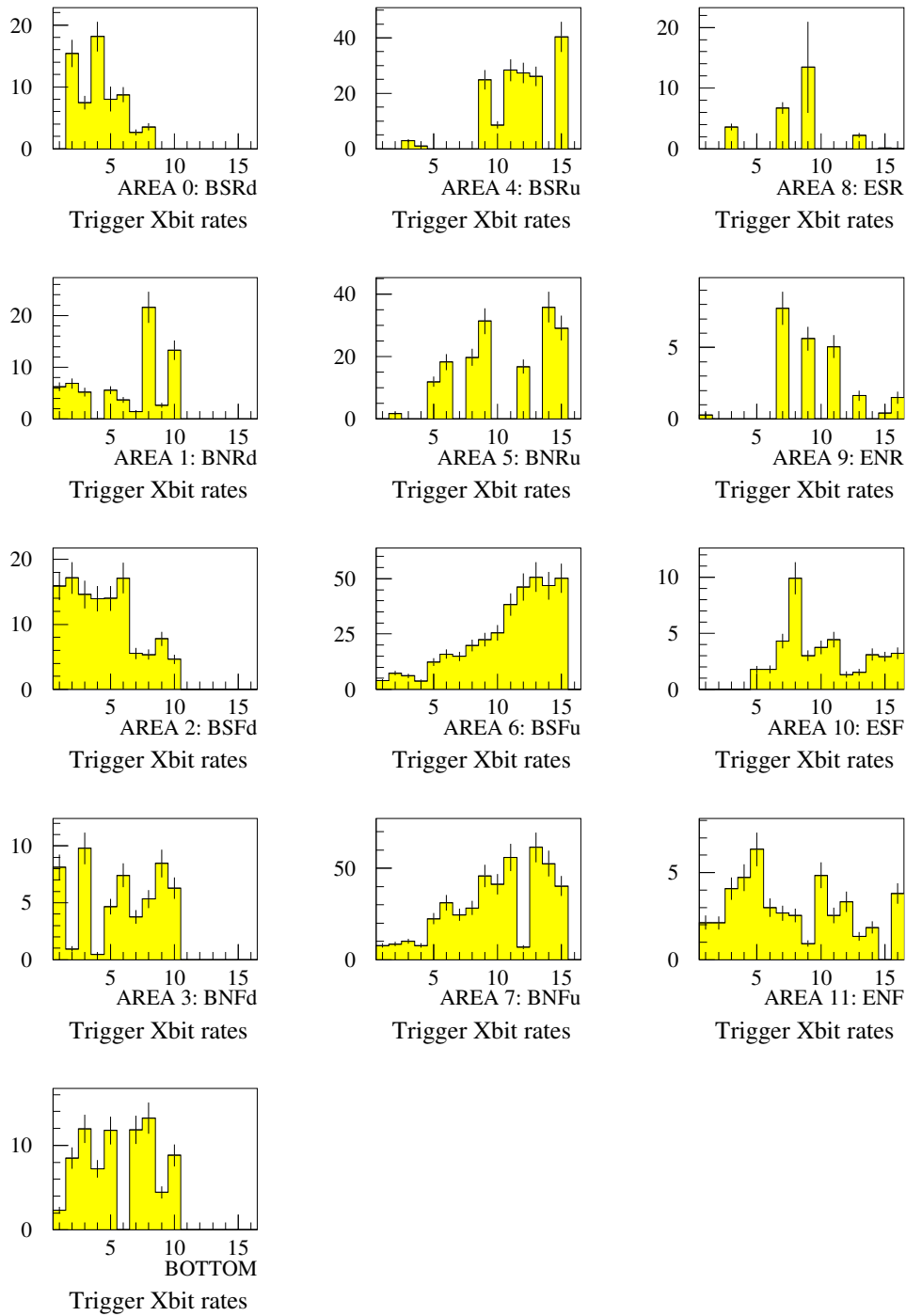
Figure 6.2: Rates of the BAC muon trigger, as measured for single wire towers in the cosmic run.

- magnets of the ZEUS experiment, solenoid and yoke, need to be at the nominal current,

- all detector components need to be switched ON (both high and low voltage),

However, trimming should be performed when there is no beam in the HERA ring, to avoid additional contribution from the beam related backgrounds (real signals from beam halo particles or particles produced in beam-gas interactions).

The trimming procedure is performed separately for the position readout (hitbox threshold trimming) and for analog readout (strip readout pedestal trimming). Adjustment of the strip readout pedestal levels is important for the performance of the BAC muon trigger in the forward direction. Due to the very high beam related background rates, coincidence of the strip and position readout is required before sending BAC trigger to GFLT.

Hitbox Trimming

Threshold trimming procedure is performed to optimize the threshold settings for 356 hitboxes, corresponding to about 40.000 position readout channels. As each hitbox contains up to 15 submodules (so called pipelines) the threshold settings for about 5000 pipelines need to be optimized. Each pipeline is directly connected to preamplifier of the BAC chamber wire readout and one threshold value is set for all connected channels (8 or 7 wires from single chamber).

The threshold trimming algorithm is the following. First, discriminator thresholds in all pipelines are set to 6 units (approximately 120 mV; one unit corresponds to about 20 mV). This reference level was found from the large sample of data collected with physics trigger. With lower threshold, trigger rate is too high for proper system performance. On the other hand, we want to keep the discriminator thresholds as low as possible, as increase of the reference threshold by one unit decreases trigger efficiency by about 5%.

In the next step, sample of 10'000 events is collected with the random trigger. Random trigger ensures that the data can be treated as "empty" events i.e. events corresponding to the noise level. The threshold trimming procedure reads the data stored in memory buffer and starts noise level checking. If the threshold is correctly set a single pipeline should not "respond" in more than few event (out of 10'000). If the noise level is higher, procedure raises the threshold for given pipeline by one unit. The step is repeated 8 times to assure that thresholds for all pipelines are correctly set.

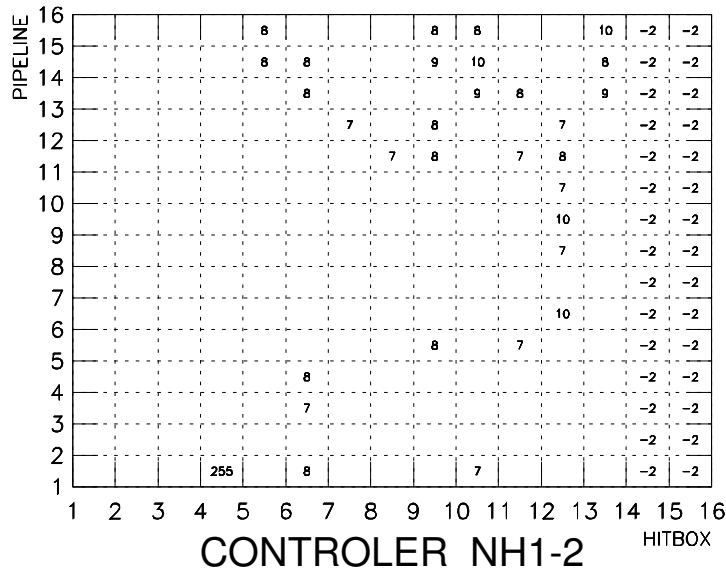| PIPELINE \ HITBOX	1	2	3	4	5	6	7	8	9	10	11	12	13	14	15	16
16					8				8	8			10		−2	−2
15					8	8			9	10			8		−2	−2
14						8			9	8			9		−2	−2
13							7		8			7			−2	−2
12								7	8		7	8			−2	−2
11												7			−2	−2
10										10					−2	−2
9												7			−2	−2
8															−2	−2
7										10					−2	−2
6									8		7				−2	−2
5															−2	−2
4						8									−2	−2
3						7									−2	−2
2															−2	−2
1				255		8				7					−2	−2

CONTROLER NH1-2

Figure 6.3: Results of the hit readout threshold trimming procedure for 13 selected hitboxes. Empty box corresponds to default threshold of 6 units. Negative threshold values (-2) are shown for unconnected hitboxes.

If the optimum threshold cannot be determined due to malfunction of the hardware or the noise level is too high a maximum threshold of 255 units is set. Such a pipeline is not read by the data acquisition system.

In addition, the threshold trimming procedure allows also for manual setting of the individual thresholds, as in some cases the threshold needs to be raised "by hand". This is because some noise is produced by external sources (other detector components), appears only during the data taking and cannot be determined by automatic threshold setting procedure described above. Results of the threshold trimming procedure are stored in the database and can be also displayed in human readable form (see Figures 6.1 and 6.3).

Strip Trimming

Similar procedure is used to find an optimal pedestal level for 133 strip towers, which allows us to separate true energy deposits from noise. As mentioned above coincidence of the muon trigger from position readout with strip energy measurement is required before sending BAC trigger to GFLT. Each channel of STT board is equipped with LTM which is used to evaluate the measured energy deposit for single strip tower. Using data collected with the random trigger mean pedestal value is extracted. The value is stored in the database
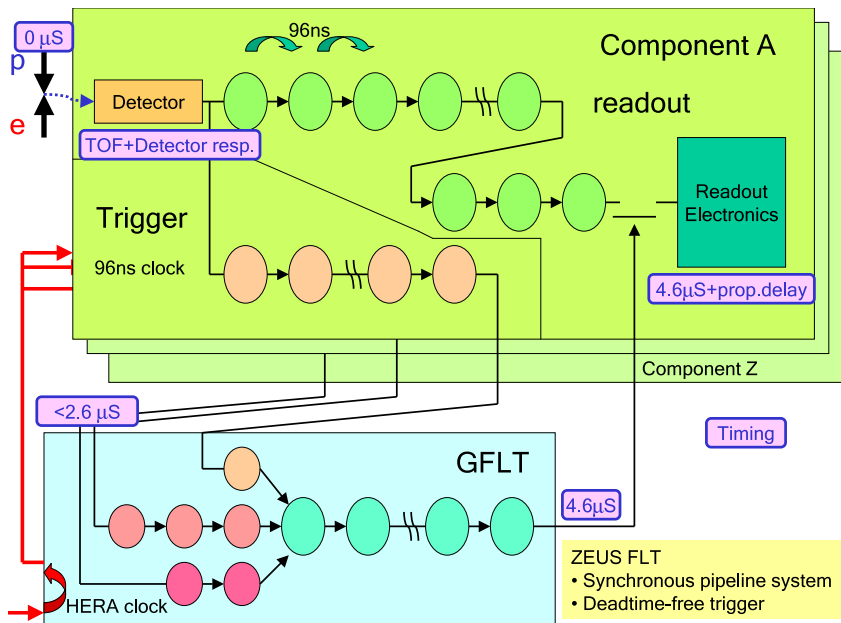
Figure 6.4: Data flow between ZEUS detector components and GFLT

and used to evaluate proper filing of the STT LTMs.

6.3 Timing adjustments

All test described so far focus on BAC hit readout and trigger electronics startup and trigger efficiency optimization. However, BAC is considered as a "stand-alone" detector and no correlation with other components is required. For the nominal ZEUS data taking, when many different components are involved, we have to assure proper internal synchronization of BAC readout components as well as BAC synchronization with GFLT to assure high BAC trigger efficiency. Proper timing of BAC trigger decision is of special importance because time required to evaluate it is much longer than the time between two subsequent beam crossings. Even small shift in trigger timing can significantly reduce trigger efficiency when requiring coincidence with other detector components.

GFLT timing requirements

According to the GFLT protocol [14] component FLT data have to be calculated within 2.5 μs (26 HERA clocks) from the corresponding beam crossing
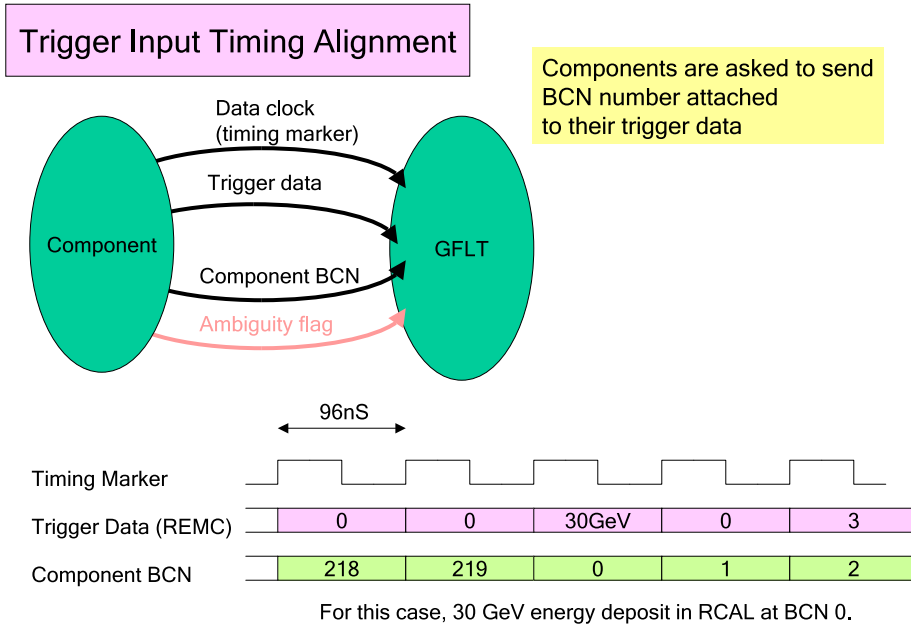
Figure 6.5: Component trigger data structure

at the interaction point. After this time trigger data are transferred to the GFLT for further processing. The design of the GFLT requires that all trigger components ship their trigger data every 96 ns, even if they are in the readout mode (processing previous GFLT "ACCEPT"), as the ZEUS FLT is designed as a deadtime free system. The GFLT gathers and matches components trigger data (see Figure 6.4). The total time available to calculate the final trigger decision at the GFLT is set to 1.9 μs (20 HERA clocks). If the event is accepted, a positive decision is distributed to all components of the ZEUS experiment exactly 46 HERA clocks after the corresponding beam crossing.

Trigger data corresponding to the same crossing are sent by various detector components at different times (26 HERA clocks is the maximum allowed delay, but components are allowed to send their data earlier). Therefore GFLT is also responsible for matching trigger data coming from different components. For this purpose, components are asked to attach their internal Bunch Crossing Number (BCN) to their trigger data (see Figure 6.5). BCN is defined as 220 cyclic number (corresponding to the bunch structure of the HERA accelerator) and its value corresponds to the time where the component FLT decision was taken and sent to GFLT. To adjust the components trigger data timing, the GFLT receives also the information about the time needed to prepare trigger decision at the component FLT level. Using this
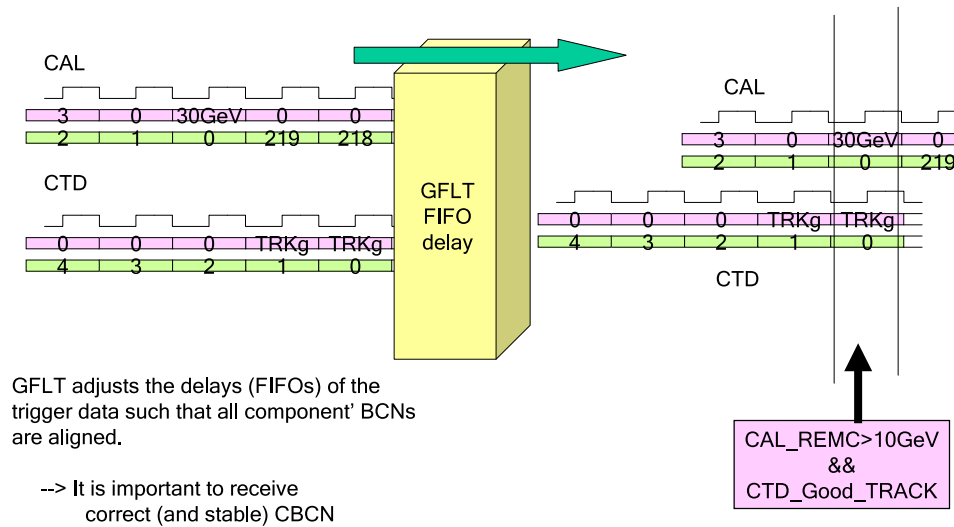
Figure 6.6: Schematic diagram of the component trigger data timing adjustment at the GFLT.

input GFLT calculates actual crossing number for each trigger data (BCN0). Based on the calculated BCN0 values GFLT matches trigger data coming from different components. The principle of trigger data time matching is presented in Figure 6.6 (for simplicity only two detector components, CAL and CTD, are considered).

For some components of the ZEUS experiment (including the Backing Calorimeter) time between the beam collision and the signal arrival at the component FLT electronics is not well defined (e.g. due to the variation of the drift time). Therefore unique assignment of BCN0 to the trigger data is not possible. In such a case components are requested to include information about the trigger ambiguity range in the data send to the GFLT. This is done by extending the component trigger decision to more than one crossing and setting the so called "ambiguity flag". The ambiguity is removed at the GFLT level by coincidence with other detector components (see Figure 6.7).

In response to ACCEPT signal from GFLT components set the BUSY signal and keep it set as long as the component is not ready to collect the next event. GFLT is not allowed to send new ACCEPT until all components finish event readout procedure and reset the BUSY signal (see Figure 6.8). Although GFLT processes trigger information continuously, some events can be missed due to detector BUSY. One of the important tasks of the GFLT is to measure the data acquisition deadtime, which contributes to the efficiency of data taking.
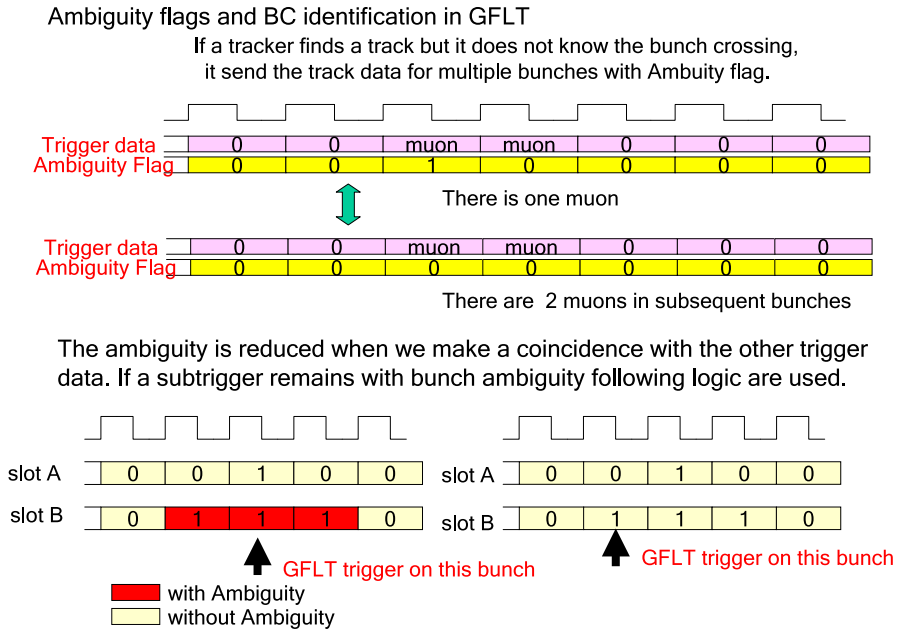
Ambiguity flags and BC identification in GFLT

If a tracker finds a track but it does not know the bunch crossing,
it send the track data for multiple bunches with Ambuity flag.

| Trigger data | 0 | 0 | muon | muon | 0 | 0 | 0 |
| Ambiguity Flag | 0 | 0 | 1 | 0 | 0 | 0 | 0 |

There is one muon

| Trigger data | 0 | 0 | muon | muon | 0 | 0 | 0 |
| Ambiguity Flag | 0 | 0 | 0 | 0 | 0 | 0 | 0 |

There are 2 muons in subsequent bunches

The ambiguity is reduced when we make a coincidence with the other trigger
data. If a subtrigger remains with bunch ambiguity following logic are used.

| slot A | 0 | 0 | 1 | 0 | 0 |
| slot B | 0 | 1 | 1 | 1 | 0 |

GFLT trigger on this bunch

| slot A | 0 | 0 | 1 | 0 | 0 |
| slot B | 0 | 1 | 1 | 1 | 0 |

GFLT trigger on this bunch

with Ambiguity
without Ambiguity

Figure 6.7: BCN ambiguity resolving at the GFLT level

GFLT

Trigger (accept flag)

CAL

busy

CTD

busy

busy

Dead time   Dead time

"event"

GFLT accept

Busy A

Busy B

Busy Z

Busy OR
(GFLT internal)
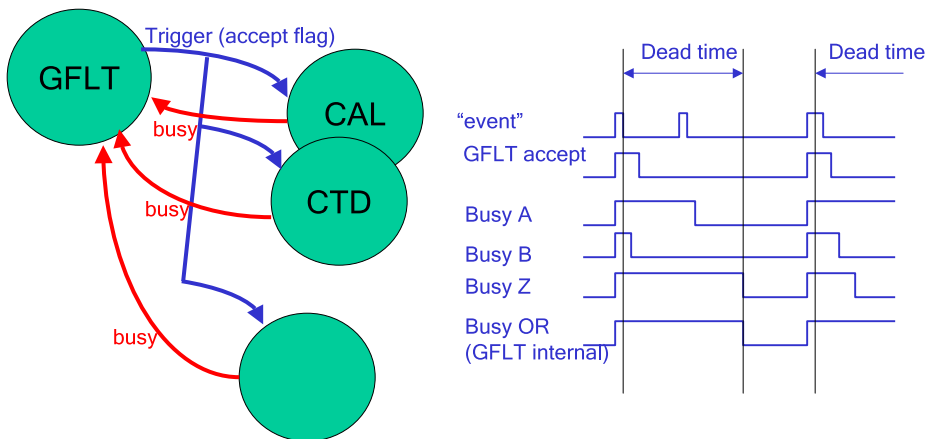
Figure 6.8: Detector readout control at GFLT level.

Timing adjustments

As mentioned in the previous chapter, the trigger components of the Backing Calorimeter have been installed in four locations: on the detector (front-end electronics), in the north and south balconies and in the rucksack. The average distance between trigger electronics parts exceeds 10 m, corresponding to signal delay of over 50 ns. Therefore we need to optimize the delay settings for each trigger channels to avoid the trigger efficiency losses. For that purpose dedicated procedure has been developed.

Timing adjustments procedure was performed using the cosmic and physics data samples as well as data collected with charge injection system. Most of the trigger electronics, in particular FPGA/ALTERA trigger boards are equipped with programmable delay time circuits. First the so called reference channel is found and the reference time is calculated for each XYREC board as:

$$T_{reference} = max(T_0, T_1, ..., T_n) \tag{6.1}$$

where: n is the number of channels and T_i is the average arrival time of selected trigger channel i. Then signals from remaining channels are delayed to match with the reference channel timing. In few cases, the difference between the reference timing and the average channel timing was greater than 400 ns. For these channels timing cannot be properly adjusted, as the circuits allow for maximum delay of 400 ns. However, the number of such channels was found to be at the level of 2 %.

Similar procedure should be performed to adjust timing between signals from XYREC boards (trigger signals from single areas) on the BMBAC board level. However, it turned out that after timing adjustments on XYREC boards level, no timing shifts between areas are observed.

Data collected with charge injection system can only be used to determine the approximate delay settings. Precise trigger timing tuning is not possible as the detector performance (charge drift inside the chamber and pulse propagation along the wire) is not taken into account in this approach. Therefore, the final adjustment of delay settings has to be done with "real" (cosmic or physics) data samples.

Data sample collected during the cosmic runs can be split into two categories: "local" i.e. BAC stand-alone cosmic runs and runs taken with full data acquisition chain of the ZEUS experiment. Local operation mode is intended for trigger performance, including trigger rate measurements and can also be used for timing adjustment studies. Final trigger timing corrections have to be evaluated using physics data samples, as the cosmic data are not synchronized with the HERA (i.e. trigger) clock.

Figure 6.9 shows the results of the timing adjustment procedure performed on the area level (XYREC board) with the physics data sample. Trigger timing distributions for single wire towers within one area, before and after adjustment procedure are compared. For each tower trigger arrival time is spread over 3 to 4 crossings. This is due to the charge drift time variations, but also to the fact that the trigger decision is extended to two crossings (ambiguity). It can be seen that after adjustment most probable trigger timing (corresponding to BCN0) for all channels is the second crossing.

Trigger timing distributions measured on the BMBAC board for selected BAC areas, before and after timing adjustment on the XYREC board level, are compared in Figure 6.10. This plot demonstrates that with the timing adjustments on the area level timing shifts between areas are also removed. The timing spread for individual areas is reduced as well.

In order to integrate the BAC trigger with the GFLT system, parameter defining the time needed to evaluate the trigger decision need be established. After several test runs performed with the use of BAC diagnostics system, this parameter was found to be exactly 20 HERA clocks.

As mentioned above, to compensate for possible drift time variations the BAC muon trigger decision was extended to 2 consecutive crossings (with ambiguity bit set to 1). However, the trigger efficiency obtained with this setup was still below expectations. After additional test runs it was decided to extend BAC trigger decision to 4 consecutive clocks. This resulted in significant increase of trigger efficiency without noticeable influence on the detector running conditions or data quality. Probability of the false BAC muon trigger, after coincidence with other detector components is very low.

6.4 Muon selection criteria

The crucial part of the muon trigger system is the programmable LTM of the position electronics which should allow us to separate muons from hadron cascades. As mentioned in previous section, the algorithm is based on the following principle: if the number of "active" layers is approximately equal to the number of "active" chambers then the event is classified as a muon and the so called X bit is set to 1. Otherwise, when the number of "active" chambers distinctly exceeds the number of "active" layers such an event corresponds to the hadron cascade and bit Y is set to 1.

The LTM filling can be represented as the two dimensional matrix, where x-axis correspond to the number of "active" chambers and y-axis correspond to the number of "active" layers. The memory filling is defined, separately
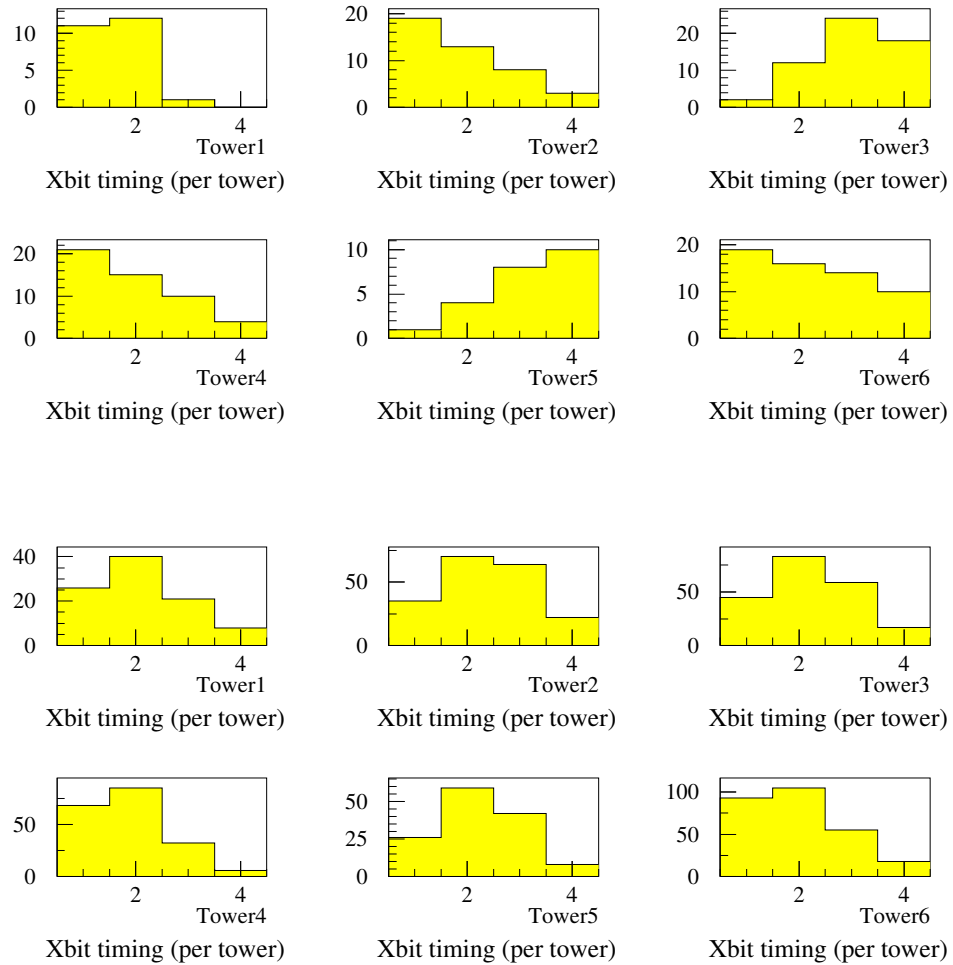
Figure 6.9: X bit timing distributions for single wire towers before (upper plots) and after (lower plots) timing adjustment procedure. Only six selected towers from one area are shown.
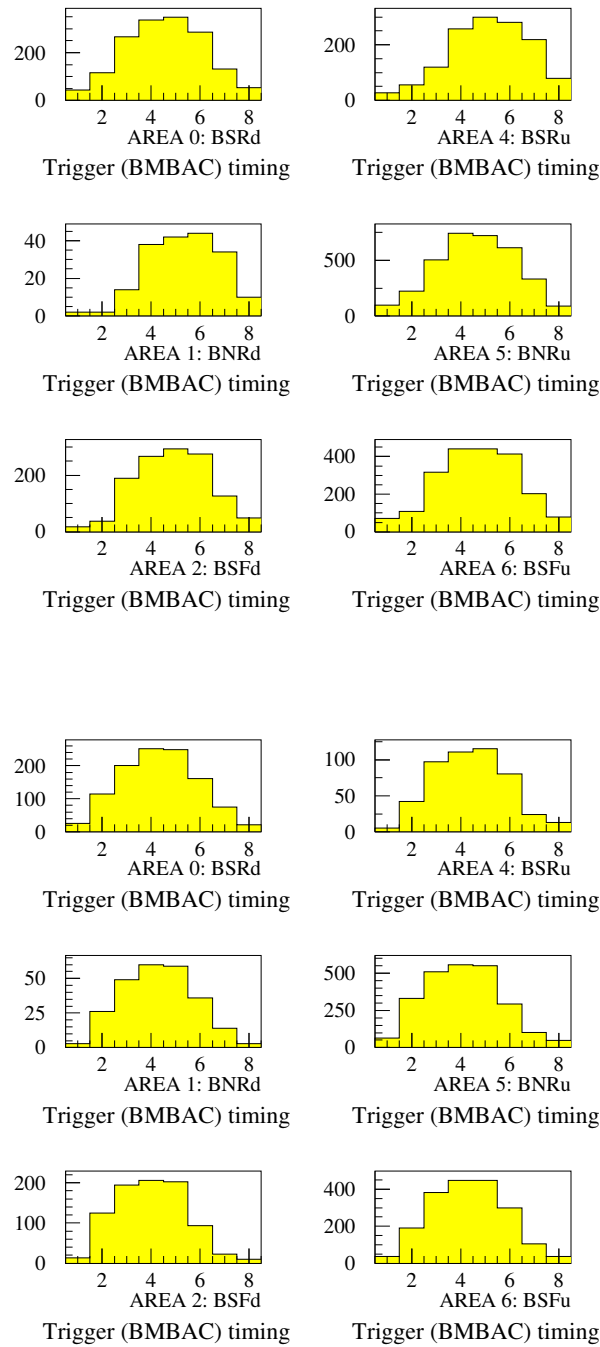
Figure 6.10: X bit timing distribution for single BAC area before (upper plots) and after (lower plots) timing adjustment procedure. Only six selected areas are shown.
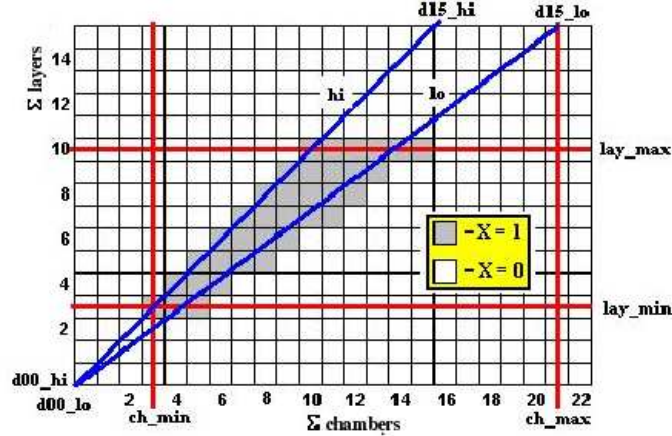
Figure 6.11: Definition of the position electronics LTM filling for X bit calculation. Filled boxes correspond to combinations of the numbers of "active" layers and "active" chambers recognized as a muon signal (bit X set to 1). Open boxes correspond to combinations not considered as a muon (bit X set to 0).

for X and Y bits, by the following parameters (see Figure 6.11):

- *lay_min* and *lay_max*: minimal and maximal number of active layers

- *ch_min* and *ch_max*: minimal and maximal number of active chambers

- *d00_hi* and *d15_hi*: points defining the straight line corresponding to the maximum number of layers for given number of chambers
  (points at which this line crosses $\sum layers = 0$ and $\sum layers = 15$)

- *d00_lo* and *d15_lo*: points defining the straight line corresponding to the minimum number of layers for given number of chambers
  (points at which this line crosses $\sum layers = 0$ and $\sum layers = 15$)

The tuning of the LTM filling is based on the analysis of the trigger variables calculated offline for selected samples of hadrons cascade, muon and "random" trigger events (empty events which corresponds to the noise level). In each case, numbers of "active" layers and chambers for single towers are calculated and then the distribution of the number of layers is plotted as a function of the number of "active" chambers. The analysis should allow us to determine optimal parameters of the LTM filling, resulting in efficient separation of muons from hadron cascades.

Distributions of the number of layers as a function of the chamber number, as obtained for three considered event samples are presented in Figure 6.12 [27]. Comparison of the two upper plots show that low energy
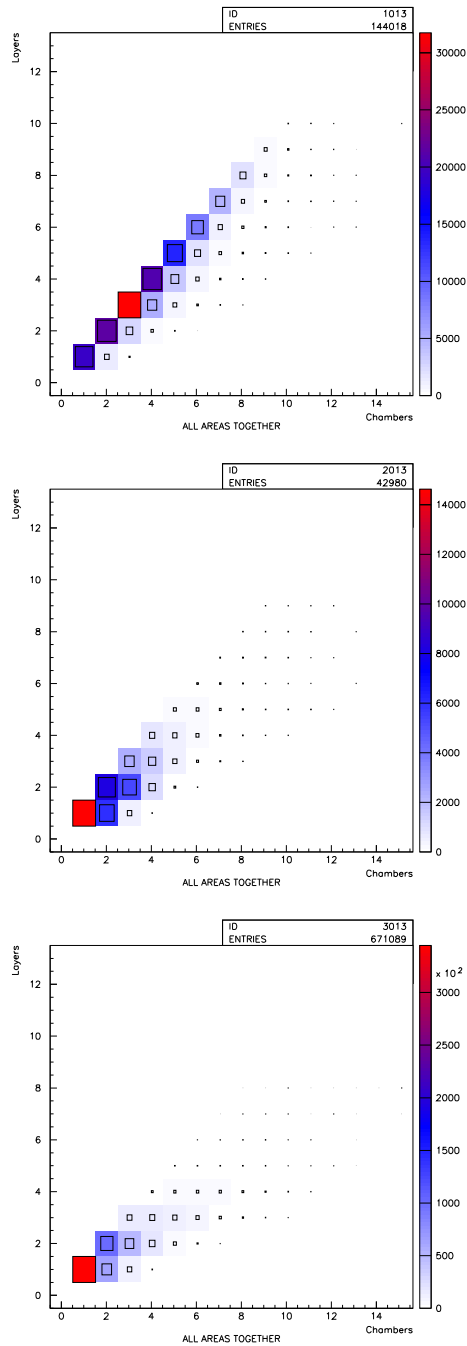
Figure 6.12: Distribution of the number of "active" layers as a function of the number of "active" chambers, as used in the BAC muon trigger algorithm, for all BAC towers. Plots correspond to the selected muon event sample (upper plot), matched hadron cascade leakages (middle plot) and random trigger events [27].
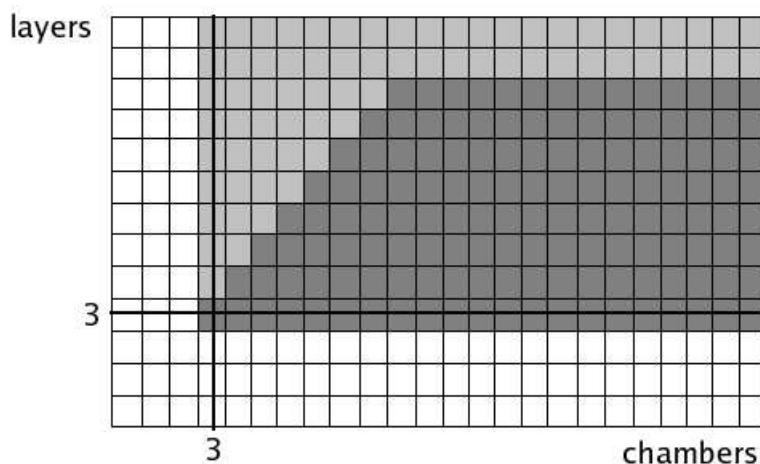
Figure 6.13: Position electronics LTM filling used for X bit calculation, as resulting from the presented analysis. Filled boxes correspond to combinations of the numbers of "active" layers and "active" chambers recognized as a muon signal (bit X set to 1). The physical range of parameters (dark fill) was extended to account for possible hardware malfunction (light fill area).

hadron cascades entering the Backing Calorimeter are likely to behave like the low energy muons. The ratio of "active" layer to chamber number is similar and only the average layer multiplicity is lower. This results show that it is not possible to separate muons from hadron cascades in the BAC FLT without significant loss of muon selection efficiency. Therefore it was decided to focus on the best separation of muon signal from the detector noise. The expected rate of contributing hadron leakages is low and they can be efficiently rejected on the BAC TLT or in off-line reconstruction, when full hit patterns are available.

The position readout LTM filling actually used in the BAC detector running is shown in Figure 6.13. To avoid any possible efficiency losses all events with at least 3 layers and 3 chambers hit are accepted as muon candidates. Also "unphysical" values of the layer and chamber numbers (e.g. number of layers greater than number of chambers or number of "active" layers greater than the actual number of layers in the detector) are accepted to account for possible hardware malfunction.

6.5 Data Quality Monitoring

In order to monitor the BAC trigger output during normal data taking (so called physics runs), dedicated online Data Quality Monitoring (DQM) system has been developed. This is a crucial part of the BAC diagnostics system because it allows us to control the quality and correctness of trigger data in the real time.

Triggers coming from GFLT can be classified as:

- "physics", reserved for events coming from *ep* collisions,

- "random", generated at empty crossings to study the detector noises,

- "tests", used to trigger the charge injection system,

- "environmental", dedicated to collect any other information sent by the component DAQ.

BAC DAQ uses the "environmental" trigger to retrieve trigger rate histograms, which are filled also during normal running conditions. The dedicated DQM process extracts a subset of the Backing Calorimeter data from the Event Builder and visualizes BAC trigger rates retrieved from the "environmental records".

Chapter 7

Trigger Performance

The main aim of the BAC muon trigger is to select events with muons produced in ep collisions. Therefore, the actual performance of the BAC FLT has to be verified on the "physics sample" i.e events used for physics analysis. The procedure should also verify if the positive decision taken on the BAC FLT level survives subsequent cuts applied on higher trigger levels and in reconstructions.

For detailed study of muon trigger performance the di-muon sample, which can be selected with high purity, is used. Di-muons originate mainly from J/Ψ production and Bethe-Heitler processes (see Chapter 2). The total integrated luminosity of the ZEUS 2005 data used in this analysis, taking only events which pass the data quality validation procedure (EVTAKE), is about 50 pb^{-1}. For comparison, Monte Carlo event samples generated with GRAPE (Bethe-Heitler processes) and HERCULES (J/Ψ production) are used. Monte Carlo samples are normalized to the data.

7.1 Event selection criteria

To avoid systematic bias in the BAC FLT efficiency estimates, we use the sample of events passing independent trigger based on the Barrel and Rear Muon chambers (BRMUON). In the off-line analysis, in order to extract pure sample of di-muons from J/Ψ decays and Bethe-Heitler process, the following cuts are applied:

- the total number of CTD tracks should be

$$1 \quad < \quad N_{trk} \quad < \quad 6$$

- to suppresses non-ep backgrounds (e.g. cosmic muon events) reconstructed vertex position along the beam line should be close to the

nominal IP

$$|z_{vtx}| \quad < \quad 50cm$$

- To rejects most of the contributing non-diffractive events the cut on the energy deposit in the hadronic section of FCAL is used

$$E_{FHAC} \quad < \quad 40GeV$$

- two good muon candidate tracks are found in CTD

$$N_{trk}^{\mu} \quad = \quad 2$$

  where a good track is defined as a track originating from the reconstructed IP, with at least 1.5 GeV/c of transverse momentum and passing at least 3 CTD superlayers. The track matching electron candidate (in NC DIS events) is not considered as a muon track candidate.

- muon tracks should have opposite charges

$$q_1 + q_2 \quad = \quad 0$$

- at least one muon track have to be well matched to the calorimeter cluster; DCA (Distance of the Closest Approach) between reconstructed CAL MIP and extrapolated track

$$DCA_{CAL-CTD} \quad < \quad 10cm$$

- we also require high reconstructed invariant mass of the muon-pair (as calculated from track momenta)

$$M_{\mu\mu} \quad \geq \quad 1.5GeV$$

After these cuts we still observe significant contribution from cosmic muon events. This is shown in Figure 7.1, where the cosine distribution of the angle between two reconstructed muon tracks is shown for data and MC sample. Cosmic muon contribution is clearly seen as the excess of events with collinear tracks. Single cosmic muon track passing close to the IP is reconstructed in the CTD as two back-to-back tracks ($\cos\theta \approx -1$). It is also possible that a track which is not passing through the IP is splitted into two tracks in reconstruction ($\cos\theta \approx +1$). To remove this background additional cut is applied on the angle between two muon tracks
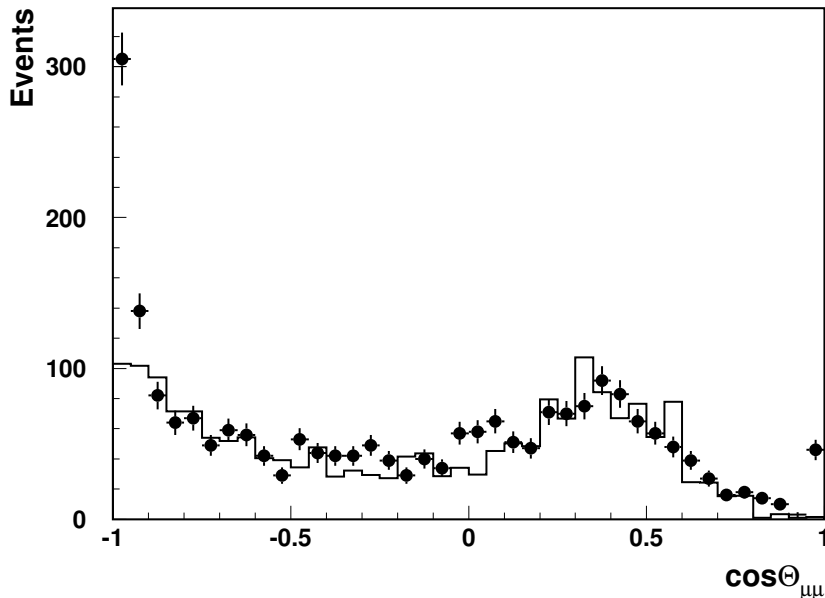
$$-0.90 \quad < \quad \cos\theta_{\mu\mu} < 0.95$$

Figure 7.1: Cosine of the angle between two reconstructed muon tracks. Selected sample of ZEUS events from 2005 running (points) is compared with Monte Carlo predictions (histogram).

After additional cut on $\cos\theta_{\mu\mu}$ very good agreement is observed between the selected sample of ZEUS events and the Monte Carlo predictions. This is illustrated in Figure 7.2, where the invariant mass distribution of two reconstructed muon tracks is shown. J/Ψ decay events and non-resonant Bethe-Heitler muon-pair production give comparable contributions to the selected event sample. Also the track momentum and polar angle distributions, as well as CTD track matching with CAL and BRMUON signals show very good agreement between data and Monte Carlo, as shown in Figures 7.3 and 7.4. Therefore, we can conclude that the selected sample of events is well understood and is appropriate for trigger performance studies.

7.2 Trigger Efficiency

As events which are not selected by any trigger slot are not stored, the efficiency of the BAC FLT can only be calculated with respect to the independent trigger of the ZEUS experiment. As mentioned above, we used
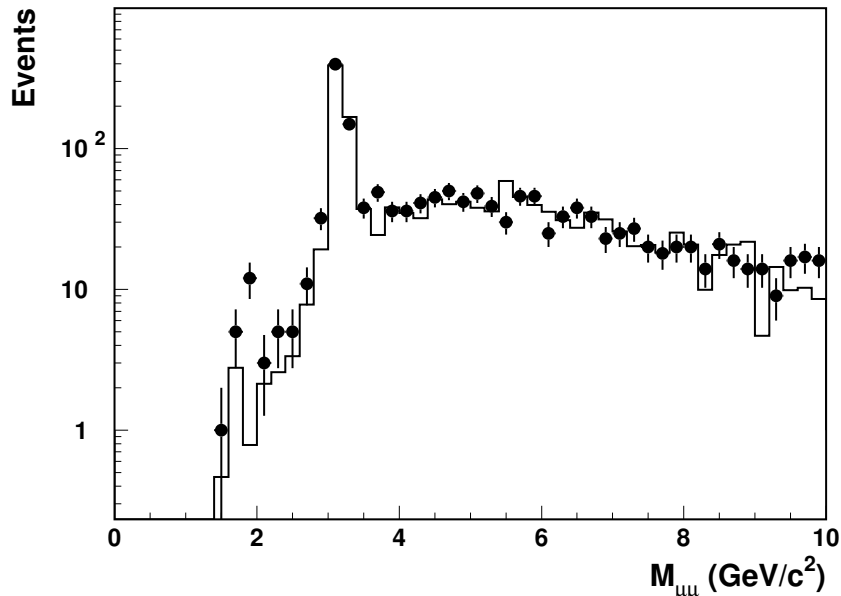
Figure 7.2: Invariant mass distribution for two reconstructed muon tracks. Selected sample of ZEUS events from 2005 running (points) is compared with Monte Carlo predictions (histogram).

data sample accepted by the BRMUON trigger system, as it should have similar geometrical and kinematical coverage as the BAC muon trigger. To confirm muon event selection in BRMUON trigger we require, that at least one muon candidate is found in the muon chambers in the off-line reconstruction. Candidate muon has to match one of the two muon tracks found in CTD. We require that the Distance of Closest Approach (DCA) between the extrapolated CTD track and the BRMUON track segment

$$DCA_{BRMUON-CTD} \quad < \quad 120cm$$

Each muon track is extrapolated to the Backing Calorimeter. We calculate the expected muon position in BAC and the ID of the corresponding trigger area. The trigger efficiency is defined as a fraction of events with the X bit (muon flag) set in the correct trigger area. This definition is a "conservative" one as the track extrapolation to BAC is not very precise (between CTD and BAC muon passes few meters in a very dense uranium calorimeter, where multiple scattering is large). For muons crossing BAC close to the area boundary extrapolation can point to "wrong" trigger area and the trigger decision is not accepted.
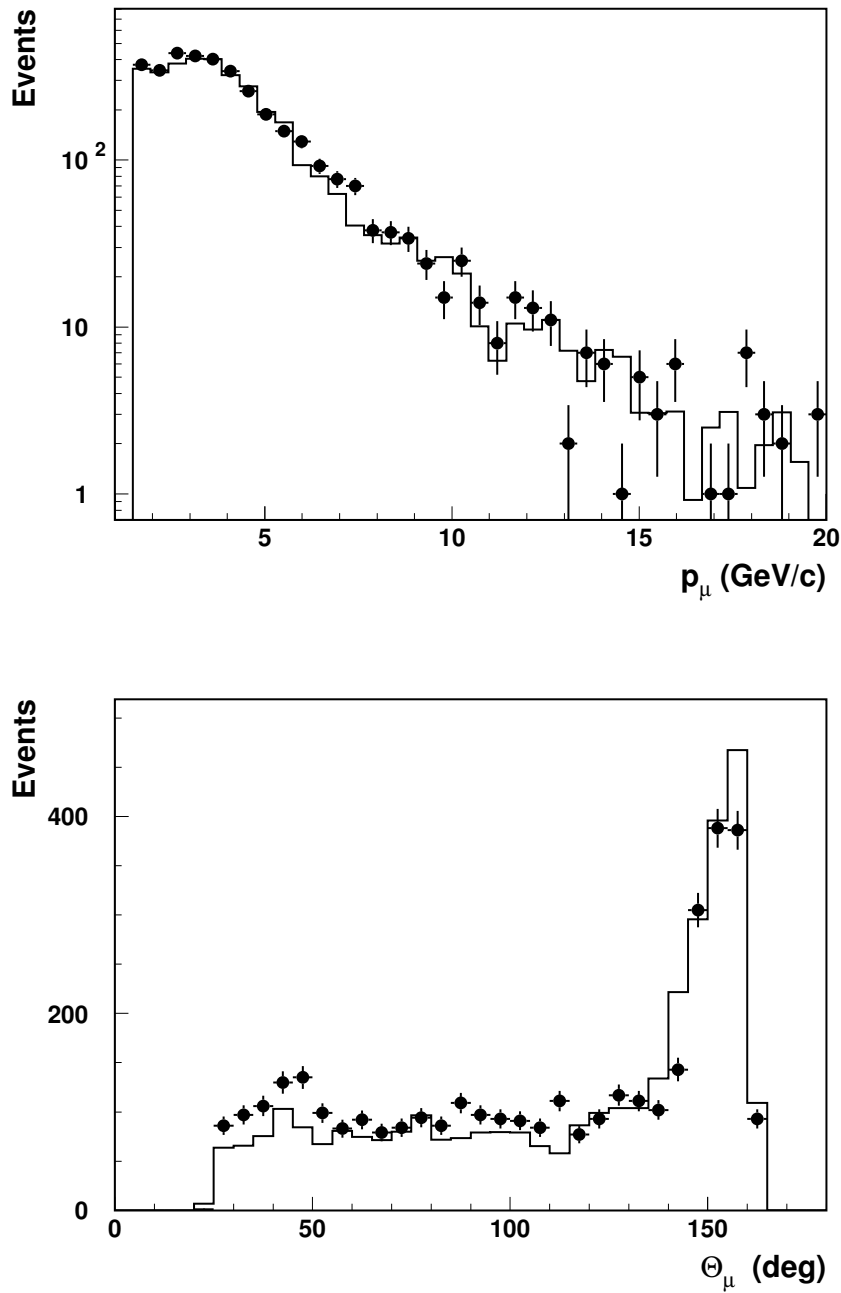
Figure 7.3: Distribution if the momenta (upper plot) and polar angle (lower plots) measured in CTD for muon tracks. Selected sample of ZEUS events from 2005 running (points) is compared with Monte Carlo predictions (histogram).
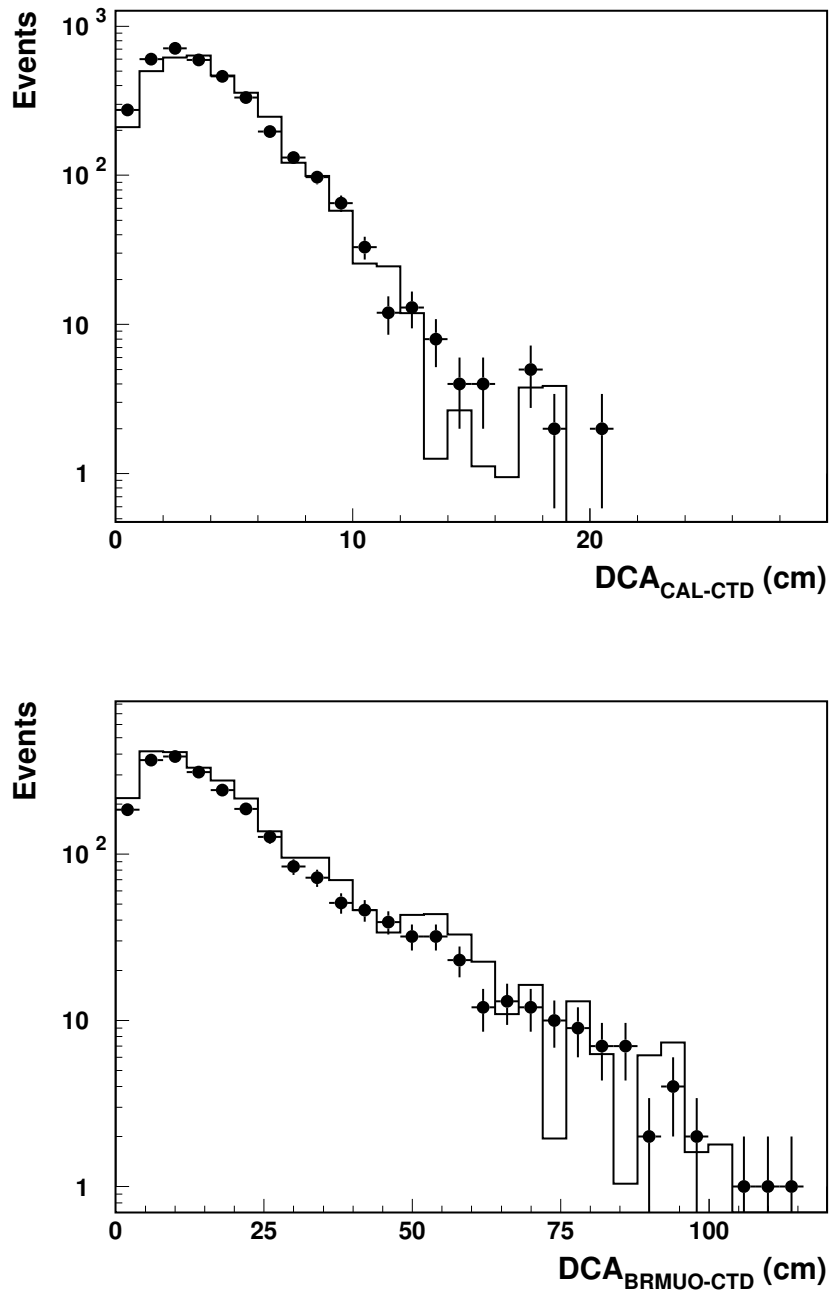
Figure 7.4: Matching between muon tracks measured in CTD and CAL (upper plot) or BRMUON (lower plot) signals. Distance of Closest Approach (DCA) distribution is shown for selected sample of ZEUS events from 2005 running (points) and Monte Carlo event sample (histogram).
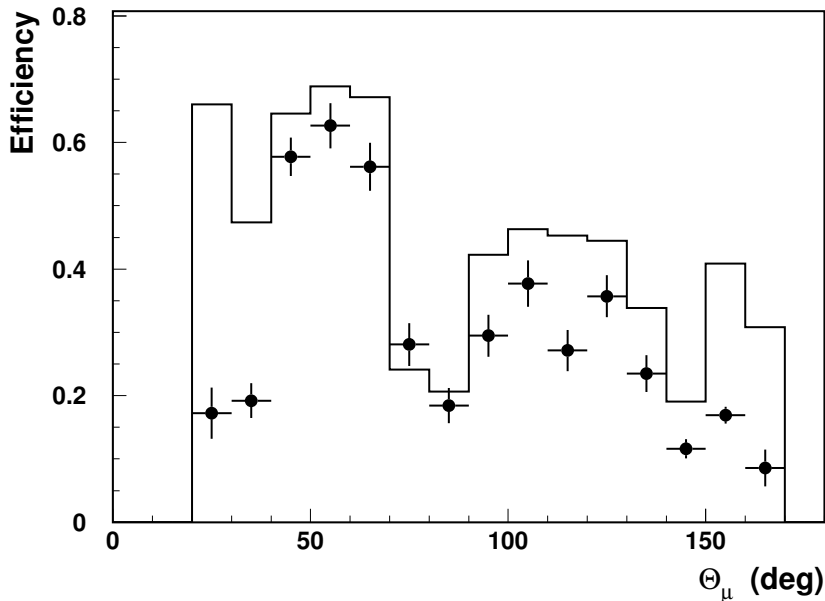
Figure 7.5: BAC muon FLT efficiency as a function of the track polar angle. Selected sample of ZEUS events from 2005 running (points) is compared with Monte Carlo predictions (histogram).

As mentioned in Chapter 6, information about the BAC FLT electronics status was stored in the database and used in the Monte Carlo simulation. Malfunctioning trigger electronics channels, as well as missing high-voltage or broken gas supply (no signal from the chamber) are taken into account. Also information about the hit readout threshold and the resulting single wire efficiency is included. However, in the current simulations software version default LTM filling is used for all trigger channels. For channels where the LTM settings had to be modified due to hardware problems (e.g. counter errors) trigger efficiency is overestimated in simulation.

Efficiency of the BAC muon FLT, for single muon tracks, as a function of the track polar angle is presented in Figure 7.5. The structure of the Backing Calorimeter is clearly visible. In the BAC Forecap ($\theta_\mu < 40°$) trigger efficiency measured in data is much lower than expected from Monte Carlo simulation. This is because, as mentioned in Chapter 6, BAC FLT decision in the Forecap has to be confirmed by the energy deposit in the strip tower. This condition is not reproduced in the Monte Carlo simulation, yet. In the Barrel part of BAC ($40° < \theta_\mu < 140°$) the dependence of trigger efficiency on

the polar angle is properly reproduced by Monte Carlo. Significant decrease of trigger efficiency in the central part of Barrel ($\theta_\mu \sim 80°$) is due three factors:

- the total length of Barrel is about 10 m. Chambers were inserted in the iron yoke from both ends (forward and read). To avoid dead region in the middle of the Barrel, different lengths of chambers were used for even and odd layers (4.5 or 5.5 m). From the trigger point of view, central part of barrel (region of overlap of longer chambers inserted from rear and from forward end) is equipped with two independent sets of chambers and trigger decision is calculated separately for even and odd layers. Trigger efficiency decreases with the number of layers;

- signal from the particle crossing BAC chamber near the chamber end is the smallest;

- muon perpendicular to the chamber ($\theta_\mu \sim 90°$) gives smaller signal than muon passing at larger angles, i.e. having longer ionization path in gas.

Discrepancy between data and simulation is again observed in the BAC Rearcap ($\theta_\mu > 140°$). This is most likely due to the BAC hardware failures (also other than the trigger electronics itself) which were not all taken into account in the Monte Carlo and different LTM settings, as mentioned above. To allow for comparison with Monte Carlo predictions, further trigger performance studies were limited to the muon tracks pointing to the Barrel BAC.

Shown in Figure 7.6 is the BAC muon FLT efficiency as a function of the muon momentum measured in CTD, for Barrel part of BAC. For low momentum tracks, below about 3 GeV/c, trigger efficiency is very low, as the track does not reach BAC. For higher momentum tracks the efficiency is approximately constant, at the level of 75% in the forward part of Barrel and about 40% in the rear part. The difference is mainly due to the fact that most of the front-end electronics in the rear part of BAC was not accessible for regular maintenance and the fraction of malfunctioning hit-boxes is much higher than in the forward part. This effect is qualitatively described in Monte Carlo.

In Figure 7.7 BAC muon FLT efficiency is shown as a function of the muon azimuthal angle, separately for forward and rear part of Barrel. Distributions in the azimuthal angle are best sensitive to the status of the individual BAC trigger channels. Monte Carlo properly describes the structure of the azimuthal angle dependence, which shows that the main information about the
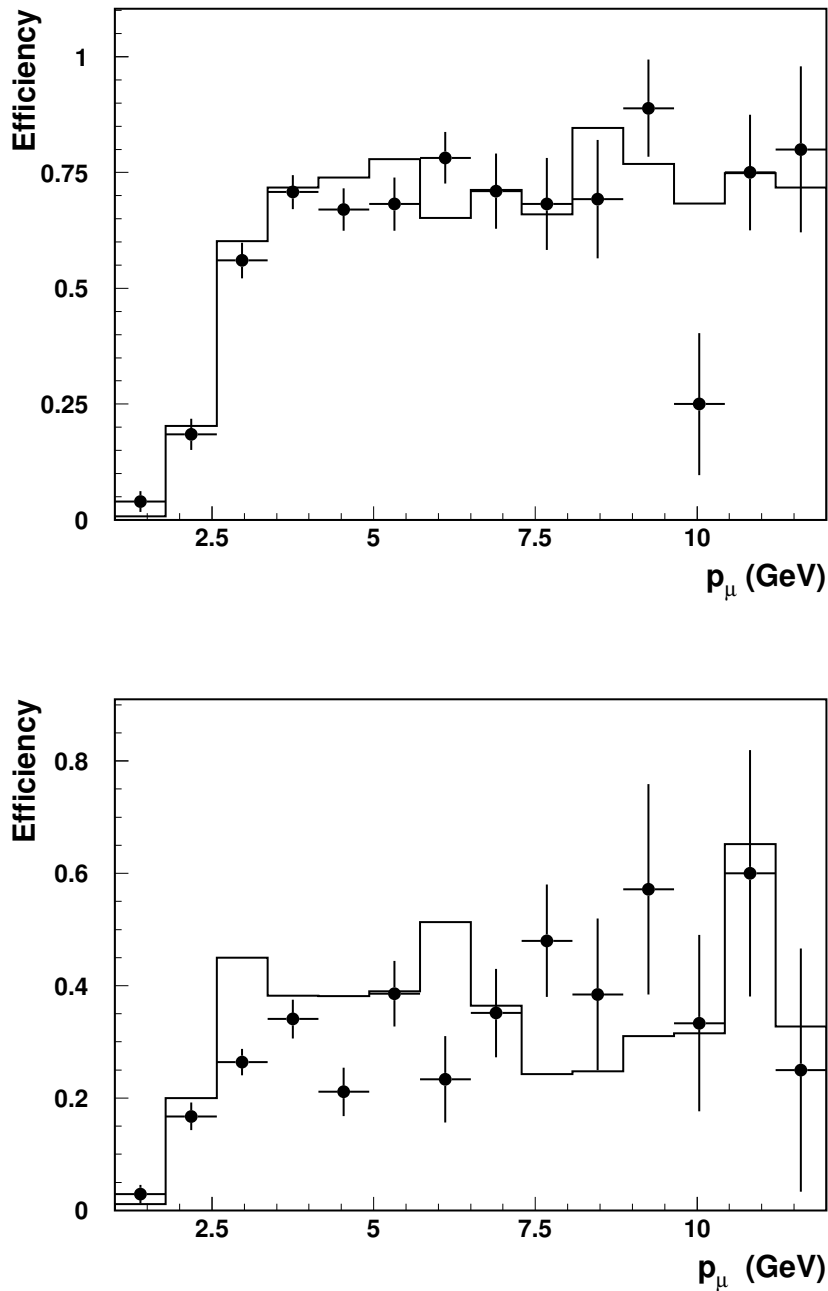
Figure 7.6: BAC muon FLT efficiency for forward (upper plot) and rear (lower plot) part of BAC Barrel as a function of track momentum. Selected sample of ZEUS events from 2005 running (points) is compared with Monte Carlo predictions (histogram).
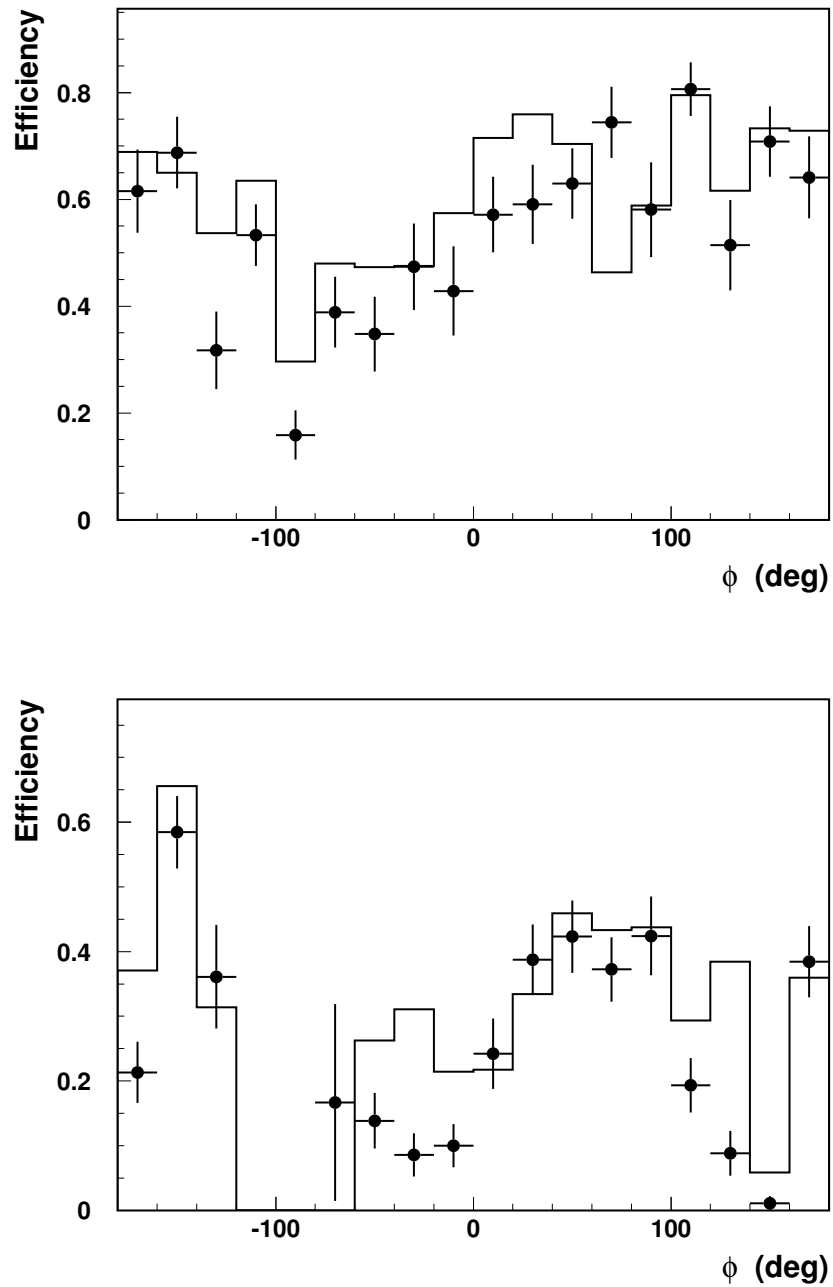
Figure 7.7: BAC muon FLT efficiency for forward (upper plot) and rear (lower plot) part of BAC Barrel as a function of track azimuthal angle. Selected sample of ZEUS events from 2005 running (points) is compared with Monte Carlo predictions (histogram).
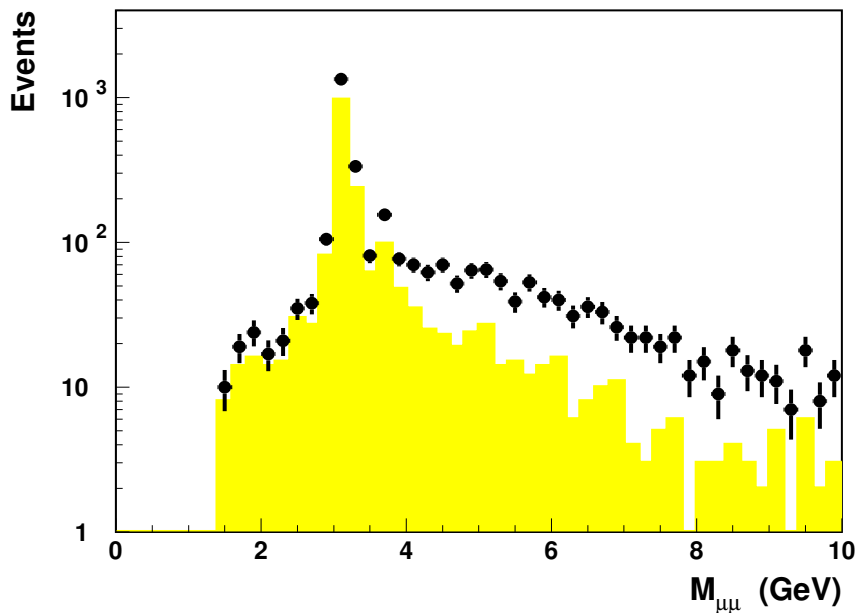
Figure 7.8: Invariant mass distribution for two reconstructed muon tracks for sample of ZEUS events from 2005 running selected with BAC FLT trigger (points). Events which were not selected by the BRMUON trigger are indicated (histogram).

BAC trigger hardware status is properly taken into account. The gap in the rear Barrel efficiency profile for $\phi_\mu \sim -90°$ corresponds to the Bottom part of BAC. Bottom is a separate area, but for simplicity it is considered as a part of forward Barrel in this analysis.

7.3 Physics Gain

All results presented so far were based on a sample of events selected with BRMUON trigger. To estimate the influence of BAC trigger on physics data analysis, we also consider sample of di-muon events selected out of all ZEUS 2005 data without setting any requirement on the trigger level (all other selection criteria, as described in section 7.1 are unchanged). This sample includes events selected by BAC FLT trigger as well as events selected by many different trigger branches (including BRMUON). We look for events with positive BAC FLT decision confirmed in the off-line analysis by a track reconstructed in the position readout matched to the CTD track.

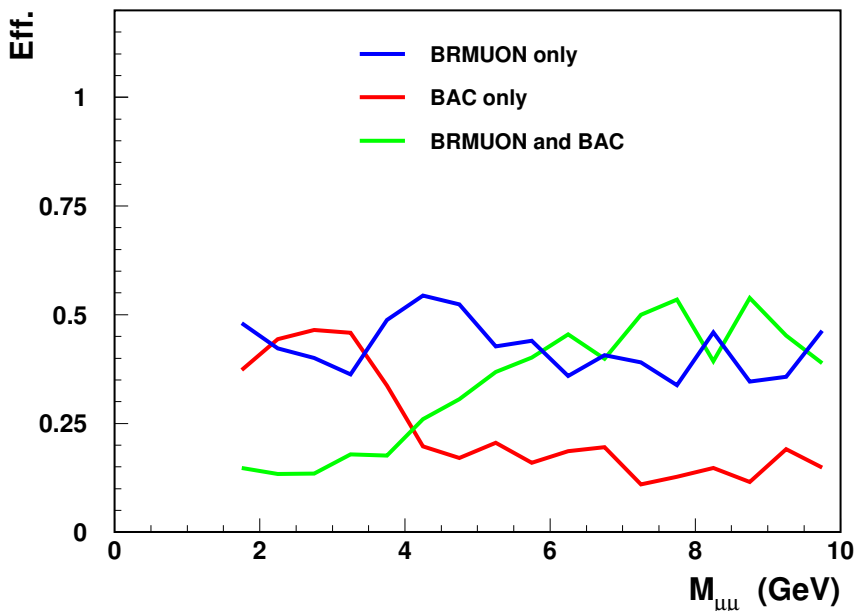Figure 7.8 shows the muon-pair invariant mass distribution for events

Figure 7.9: Fraction of di-muon events selected by BRMUON or BAC trigger only, and by both triggers, as a function of the muon pair invariant mass. Sample of ZEUS events from 2005 running selected with BAC or BRMUON FLT is considered.

selected by BAC muon trigger. Also indicated (yellow histogram) are events which were accepted by BAC FLT but failed to pass BRMUON trigger. In the region of low invariant masses most of events are selected by BAC muon trigger only.

However, we also have to take into account the possibility that event is selected by BRMUON only. Shown in Figure 7.9 are fractions of di-muon events selected by BRMUON or BAC trigger only, and by both triggers, as a function of the muon pair invariant mass. Only events selected by at least one of the two triggers are considered. The plot shows that in the region of low invariant masses (J/Ψ) BAC muon trigger can improve muon event selection efficiency by almost a factor of two. The total statistics of the di-muon sample increases by about 50%. Effect of including BAC FLT is smaller at high invariant masses, when muons with large momenta are more likely to penetrate to the outer BRMUON chambers located outside the iron yoke. Gain in the statistics of the di-muon sample is about 20% in this region. Fraction of events accepted by both triggers increases with the di-muon invariant mass.

Examples of events selected by BAC FLT are shown in Figures 7.10-7.13.

ZEuS Run 52258 Event 28843   date: 6-12-2004   time: 02:53:18

E=5.72 GeV E_t=3.15 GeV $E-p_z$=3.85 GeV E_f=3.1 GeV E_b=1.79 GeV

E_r=0.835 GeV p_t=0.534 GeV p_x=0.465 GeV p_y=0.263 GeV p_z=1.87 GeV

phi=0.52 t_f=-2.99 ns t_b=0.54 ns t_r=3.25 ns t_g=-1.13 ns

FLT= 8 10 12 14

SLT= HFL/MUO: 22 23 29 GTT: 05

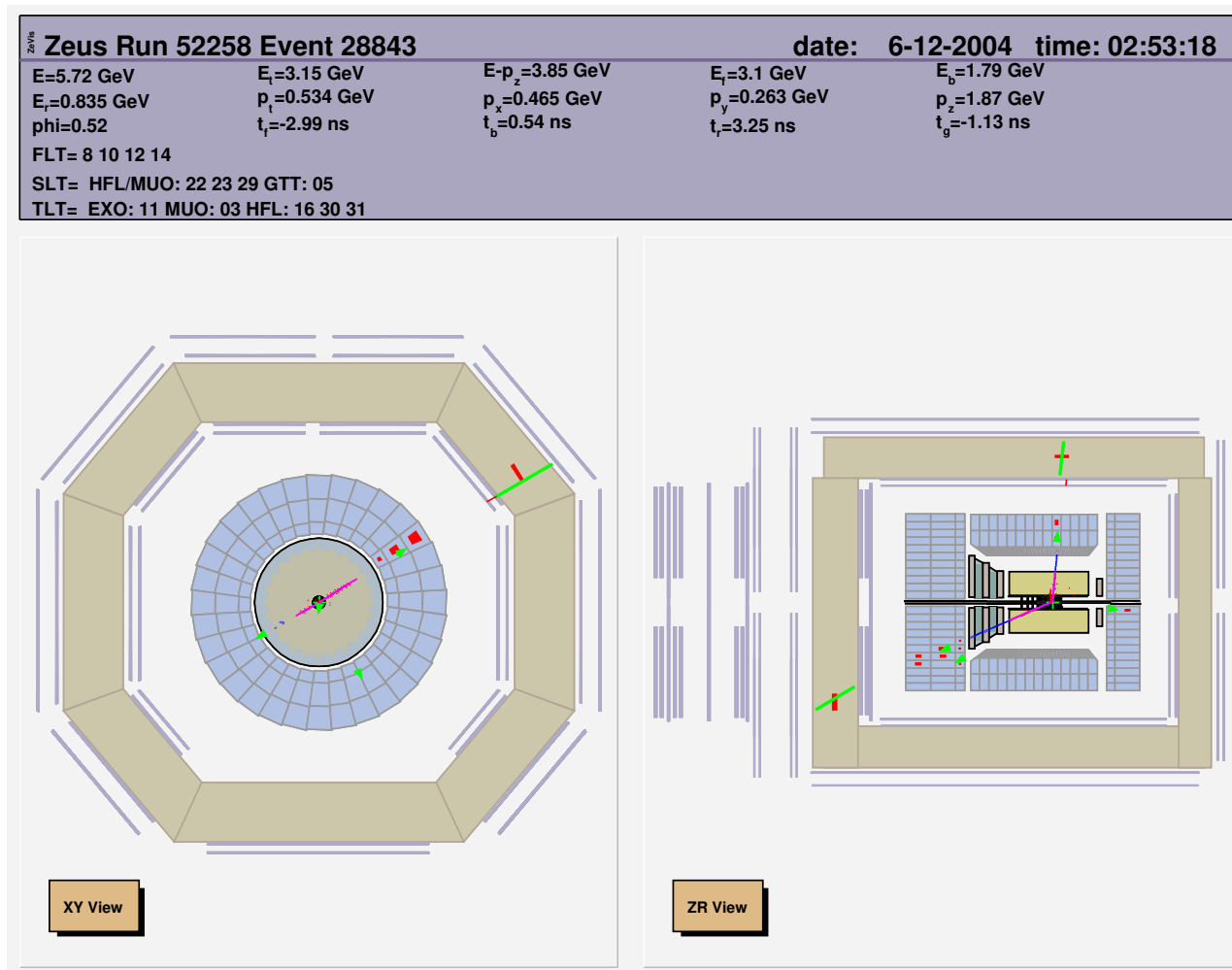TLT= EXO: 11 MUO: 03 HFL: 16 30 31

XY View

ZR View

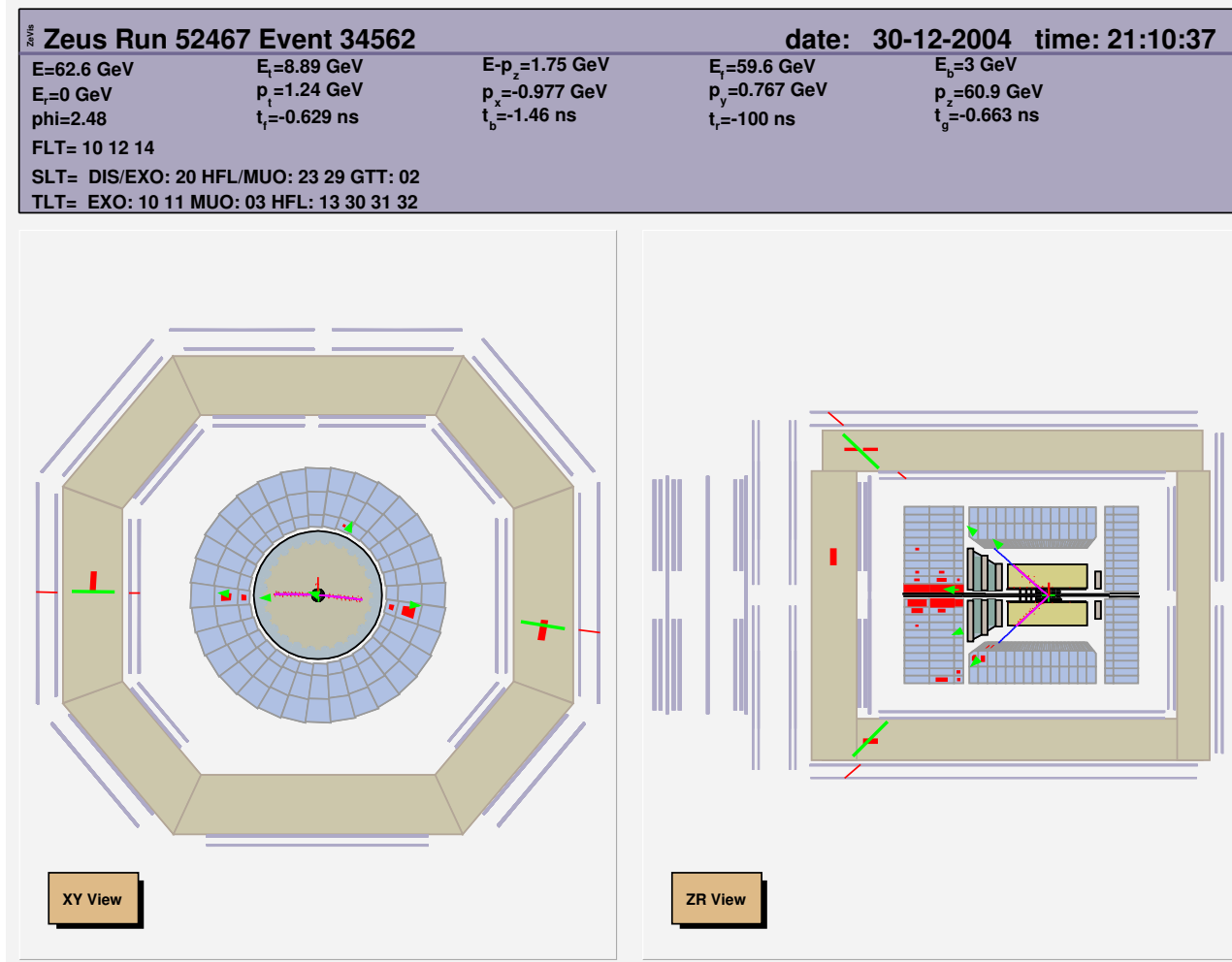Figure 7.10: Di-muon event from ZEUS 2004 data selected by BAC FLT.

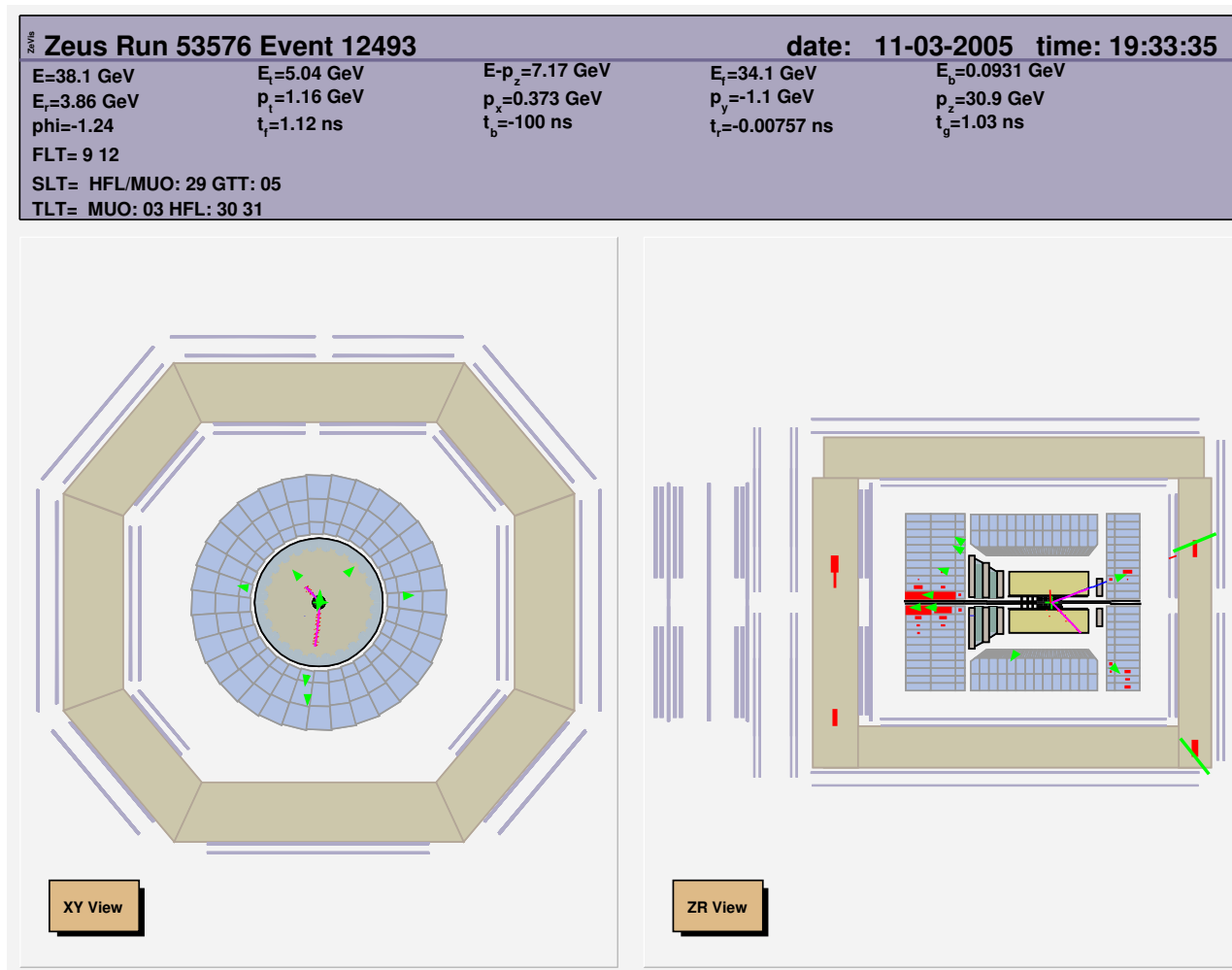Figure 7.11: Di-muon event from ZEUS 2004 data selected by BAC FLT.

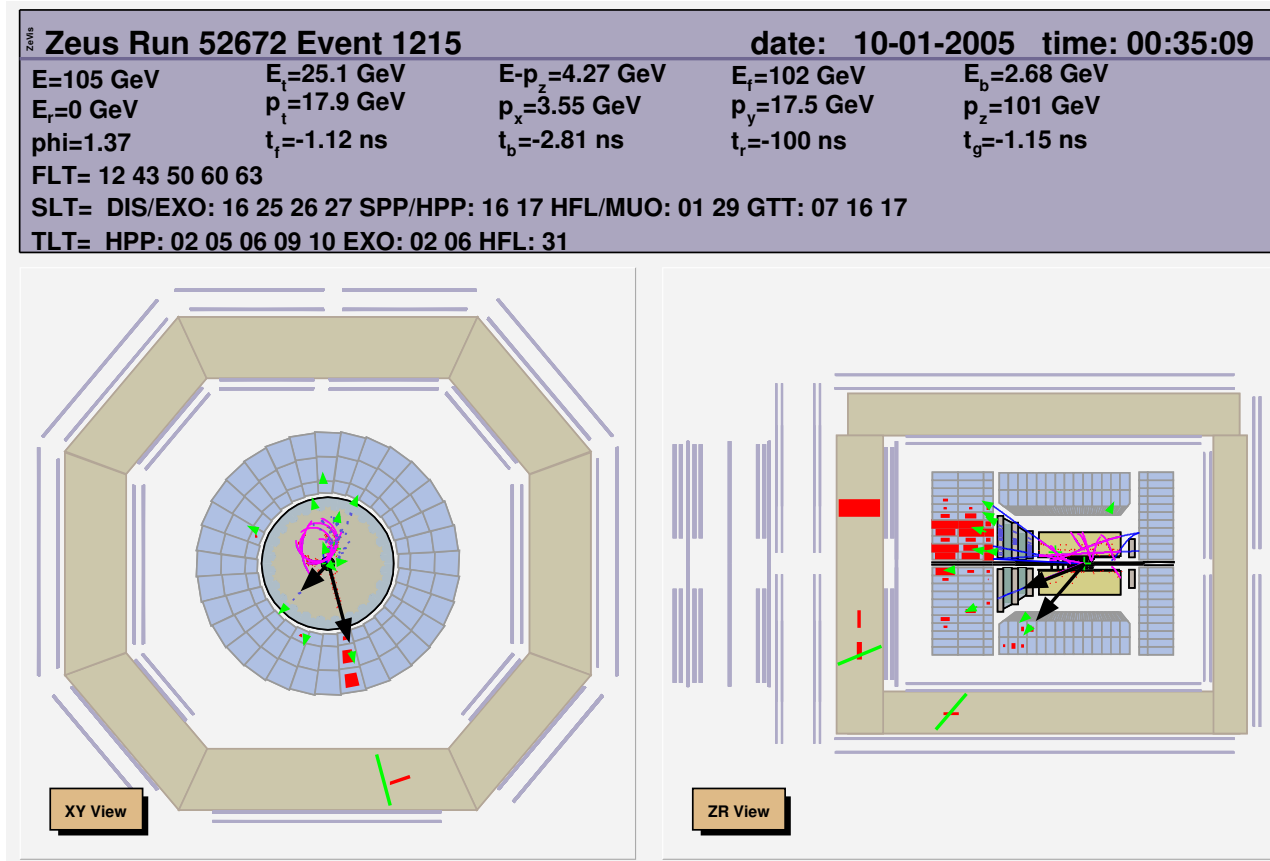Figure 7.12: Di-muon event from ZEUS 2005 data selected by BAC FLT.

Figure 7.13: Di-muon event from ZEUS 2005 data selected by BAC FLT.

Chapter 8

Summary and Conclusions

One of the most important results from HERA 1994-2000 running was the excess of events with jet and high-p_T isolated leptons reported by H1, but not confirmed by ZEUS. Therefore, an important goal of the ZEUS detector upgrade in 2000-2002 was to increase the efficiency of muon identification on the trigger level. This was obtained by implementing the muon trigger in the Backing Calorimeter. This thesis summarize the work which was done in years 2000-2006 to setup, startup and optimize the performance of the BAC muon trigger.

The Backing Calorimeter trigger system design is based on many different hardware components, placed at different locations in the experiment. The degree of complexity of this system is such that the startup and optimization procedure had to be performed in many steps.

As the first step, dedicated diagnostic system has been developed to monitor performance of the trigger system on all hardware and software levels. Detailed tests in well controlled conditions are possible as most of the readout and trigger electronics boards involve programmable circuits and LTMs. Information about the status of system components can be used to select optimum configuration parameters. Stored in the database, it is also used to reproduce performance of the BAC muon trigger in the ZEUS Monte Carlo.

The second phase of the setup procedure was the trimming of BAC position and strip readout thresholds. Threshold adjustment for individual readout channels is required to obtain best possible trigger efficiency and separation of the real particle signal from the chamber or electronic noise.

In the next step, timing of the trigger electronics, i.e. delay of the decisions coming from different BAC areas had to be adjusted to match with the requirements of the ZEUS Global First Level Trigger. Proper timing of BAC trigger decision is of special importance because time required to evaluate it is much longer than the time between two subsequent beam crossings. Even

small shift in trigger timing can significantly reduce trigger efficiency when requiring coincidence with other detector components. To compensate for possible time variations and assure highest possible trigger efficiency it was decided to extend the BAC muon trigger decision to 4 consecutive crossings.

The last step of the setup and startup procedure was related to the determination of the optimal parameters for the LTM filling, which was supposed to result in efficient separation of muons from hadron cascades. However, analysis of collected data showed that low energy hadron cascades entering the Backing Calorimeter often behave like the low energy muons. It turned out that it is not possible to separate muons from hadron cascades in the BAC FLT without significant loss of muon selection efficiency. Therefore it was decided to optimize the LTM filling for the best muon and noise separation.

Sample of di-muon events selected from ZEUS 2005 data was used to verify BAC trigger simulation and to study trigger performance. Analysis shows that, in the regions where there were no major hardware problems, BAC trigger selection efficiency for high momentum muons is about 70 to 80%. Results are well reproduced by Monte Carlo confirming that performance of the BAC muon trigger is well understood. By including BAC muon trigger in the ZEUS trigger system efficiency for high-mass di-muon event selection was increased by about 20%.

Results presented in this thesis show that the BAC muon trigger has been successfully implemented and the collected data can be used in physics analysis. Some more work is still needed to improve description of BAC hardware and trigger configuration in the simulation. Proper description of the detector status and full understanding of its performance requires detailed off-line analysis of all collected ZEUS data. However, this is a task for a separate study.

In the coming years many new physics results from HERA experiments are still expected. For HERA II integrated luminosity of almost 400 pb^{-1}, about 270 pb^{-1} of data were collected with BAC FLT and about 200 pb^{-1} with all three levels of BAC trigger implemented. This corresponds to the significant gain in statistics of collected muon events for physics studies. BAC muon trigger can be used in muon pair selection, but also for searches of isolated muons with large missing p_T or in b quark studies. Moreover, independent trigger system is an important tool for verifying our understanding and simulation of the BRMUON system.

Acknowledgments

This thesis could not have been written without the effort of many people, both inside and outside the ZEUS collaboration. I wish to thank all of them, in particular the DESY Directorate for hospitality during my stay at DESY.

Special thanks go to the following people: to prof. dr hab. Aleksander Filip Żarnecki (my supervisor) and dr Grzegorz Grzelak (BAC trigger project leader) for initiating this thesis, patience and encouragement, sharing their knowledge and supplying so much invaluable information, for all the explanations and for all interesting discussions; to prof. dr hab. Jacek Ciborowski (BAC group leader) for giving me the opportunity to work within the ZEUS Backing Calorimeter group on the muon trigger project and also to the whole ZEUS collaboration for the great working atmosphere.

Finally, special thanks go to my family and friends, for their support and to Krystyna, my wife for her trust in my work.

Bibliography

[1] HERA Collaboration, "Annual Report" Status Report (unpublished), DESY, 1994.

[2] ZEUS Collaboration, "ZEUS a Detector for HERA", Status Report, ed. Uwe Holm, Feb. 1993,
available on `http://www-zeus.desy.de/bluebook/bluebook.html`.

[3] H1 Collaboration, I. Abt et al, Nucl. Instrum. Meth. A 386 310 and 348 (1997); R.D. Appuhn et al, Nucl. Instrum. Meth. A 386 397 (1997).

[4] HERMES Collaboration, K. Ackerstaff et al., "The HERMES Spectrometer", Nucl. Instrum. Meth. A417 (1998) 230-265.

[5] HERA-B Collaboration, "Technical Design Report", Status Report (unpublished), DESY-PRC, 1995.

[6] H1 Collab., V. Andreev et al., "Isolated electrons and muons in events with missing transverse momentum at HERA", Phys. Lett. B561 (2003) 241, 01/03.

[7] E. Koffeman, "A silicon Micro Vertex Detector for the ZEUS Experiment", Nucl. Instrum. Methods A. 453 (2000) 89.

[8] ZEUS Collaboration, B. Foster et al., "The Design and Construction of the ZEUS Central Tracking Detector", Nucl. Instrum. Meth. A338 (1994) 254-283.

[9] M. Derrick et al., "Design and Construction of the ZEUS Barrel Calorimeter", Nucl. Instrum. Meth. A309 (1991) 77-100;
ZEUS Barrel Calorimeter Group Collaboration, A. Bernstein et al., "Beam Tests of the ZEUS Barrel Calorimeter", Nucl. Instrum. Meth. A336 (1993) 23-52;
ZEUS Calorimeter Group Collaboration, A. Andresen et al., "Construction and Beam Test of the ZEUS Forward and Rear Calorimeter", Nucl. Instrum. Meth. A309 (1991) 101-142.

[10] G. Abbiendi et al., Nucl. Inst. Meth. A 333, 342 (1993).

[11] H. Abramowicz et al., "Intercalibration of the ZEUS high-resolution and backing calorimeters", Nucl. Inst. Meth. A 313, 126 (1992).

[12] G. Grzelak at. el., "Overview of the Backing Calorimeter after the ZEUS detector upgrade", Proceedings of SPIE, Belling-ham, WA, USA, Vol. 5125, 2003

[13] P. Plucinski et al., "Trigger of the Backing Calorimeter for Zeus Experiment", Proceedings of SPIE, Belling-ham, WA, USA, Vol. 5125, 2003.

[14] K. Tokushuku, "GFLT Design Document I interface to component (ver. 5.1)" (unpublished) 1990.
W. Smith, K. Tokoshuku, L. Wiggers, "Global First Level Trigger Timing", ZEUS-Note-90-011, 1990.

[15] H. Uijterwaal, "The Global Second Level Trigger for ZEUS", PhD thesis, DESY, 1992.

[16] ZEUS TLT Group Collaboration, D. C. Bailey et al., "The ZEUS Third Level Trigger Hardware Architecture", Presented at International Conference on Open Bus Systems 92, Zurich, Switzerland, 13-15 Oct 1992.

[17] S. Silverstein et al., "The ZEUS Calorimeter First Level Trigger", Nucl. Instrum. Meth. A360 (1995) 322-324.

[18] INMOS Ltd, "Transputer Reference Manual", Prentice Hall 1988.

[19] W. O. Vogel et al., "The Eventbuilder of the ZEUS Detector", Prepared for 8th Conference on Computing in High-energy Physics: Computing for High Luminosity and High Intensity Facilities, Santa Fe, New Mexico, 9-13 Apr 1990.
U. Behrens et al., "The Eventbuilder of the ZEUS experiment", DESY preprint 93-008.

[20] "ADAMO: User guide", CERN, 1993.

[21] J.M. Pawlak, J. Milewski, "The design of ZEUS Data Acquisition System and Trigger Sytem", Real Time Comp. Appl. 1993; 450-454.

[22] L. Bauerdick et al., "The Physics Analysis Enviroment of the ZEUS Experiment", DESY-95-236

[23] R. Brun et al., "GEANT 3.13", CERN DD/EE/84-1.

[24] M. Kudla, R. Kupczak, K. Pozniak et al., "GFLT signal testing and distribution within the BAC system", ZEUS-Note 96-116, 1996.

[25] H. Boterenbrood, "User Software Documentation 2TP-VME Module", NIKHEF 1990.

[26] K. Pozniak, "Software control and testing of the HIT-READOUT for the BAC detector", ZEUS-Note 96-117, 1996.

[27] J. Malka, "Analiza działania układu wyzwalania kalorymetru uzupel-niajacego BAC w eksperymencie ZEUS", M.Sc. thesis (in Polish).